JOURNAL OF GEOPHYSICAL RESEARCH, VOL. 101, NO. B2, PAGES 3139-3156, FEBRUARY 10, 1996

Poisson's ratio and crustal seismology

Nikolas I. Christensen

Department of Earth and Atmospheric Sciences, Purdue University, West Lafayette, Indiana

Abstract. New measurements of compressional and shear wave velocities to hydrostatic pressures of 1 GPa are summarized for 678 rocks. Emphasis was placed on obtaining high-accuracy velocity measurements, which are shown to be critical in calculating Poisson's ratios from velocities. The rocks have been divided into 29 major groups for which velocities, velocity ratios, and Poisson's ratios are presented at several pressures. Observed Poisson's ratios for the monomineralic rocks compare favorably with theoretical Poisson's ratios calculated from single-crystal elastic constants. Plagioclase feldspar composition is important in understanding rock Poisson's ratios, since Poisson's ratio of albite increases from 0.28 to a predicted value of 0.31 for anorthite. Fe substitution for Mg in pyroxene and olivine also increases Poisson's ratio. Plotting rock compressional wave velocities versus Poisson's ratios reveals a triangular distribution bounded by quartzite with low compressional wave velocity and low Poisson's ratio, dunite with high compressional wave velocity and intermediate Poisson's ratio, and serpentinite with low compressional wave velocity and high Poisson's ratio. For common plutonic igneous rocks, there is a clear trend relating Poisson's ratio to composition, in which Poisson's ratio for granitic rocks increases from 0.24 to 0.29 as composition changes to gabbro and then decreases with decreasing plagioclase and increasing olivine contents to 0.25 in dunite. Changes in Poisson's ratio with progressive metamorphism of mafic and pelitic rocks correlate reasonably well with mineral reactions. There is no simple correlation between Poisson's ratio and felsic and mafic rock compositions; however, a linear correlation of increasing Poisson's ratio with decreasing SiO_2 content is observed for rocks with 55 to 75 wt % SiO_2. Average Poisson's ratios for continental and oceanic crusts are estimated to be 0.265 and 0.30, respectively.

Introduction

The importance of seismological determinations of Poisson's ratio values at various crustal levels is primary for understanding the petrologic nature of the Earth's crust. Early crustal seismic investigations often reported Poisson's ratios [e.g., *Gutenberg*, 1959]. These studies were seldom utilized, however, in a determinative manner other than as general constraints, for example, when observed values deviated appreciably from the commonly assumed value of 0.25. As laboratory-based compressional and shear wave velocity measurements for common rock types became available, it became apparent that a Poisson's ratio of 0.25, although approximately representative of some rocks, was based on a theoretical conception of matter bearing little relation to reality. Poisson's ratios determined from field measurements thus have the potential of providing valuable constraints on crustal composition. This is particularly important because the correlation between compressional wave velocity and composition is limited due to the similar compressional wave velocities of many common crustal rock types [e.g., *Birch*, 1960, 1961; *Christensen and Mooney*, 1995].

Recognizing the nonuniqueness of compressional wave velocity laboratory and field data comparisons, several papers have focused on investigations of crustal composition using Poisson's ratio. These studies include investigations of oceanic crustal petrology [e.g., *Christensen*, 1972; *Spudich and Orcutt*, 1980], as well as estimates of continental crustal composition [e.g., *Christensen and Fountain*, 1975; *Holbrook et al.*, 1988; *Johnson and Hartman*, 1991; *Zandt and Ammon*, 1995].

The subject of this paper is the use of Poisson's ratio to place constraints on continental crustal composition. I first review studies of single-crystal elasticity of common rock-forming minerals, which are important in understanding rock Poisson's ratios. Important trends in Poisson's ratio with the chemistries of mineral solid solution series are discussed. A summary of Poisson's ratios for common rock types follows, with averages and standard deviations tabulated from a new data set which has been subdivided into 29 major rock types. Emphasis is placed on igneous and metamorphic rock properties. For a summary of Poisson's ratios of common sedimentary rocks, the reader is referred to the studies of *Wilkens et al.* [1984] and *Johnston and Christensen* [1992]. Finally, I examine the use of Poisson's ratio in placing constraints on crustal composition.

Rocks as Mineral Aggregates

If a rock cylinder undergoes tension or compression along its axis, its diameter (d) will change in the direction perpendicular to its length (l). Poisson's ratio (σ), the ratio of radial contraction to axial elongation, is defined as $-(\Delta d/d)/(\Delta l/l)$. Values of Poisson's ratio for solids theoretically fall between 0 and 0.5. Materials without rigidity (e.g., perfect liquids), as

Paper number 95JB03446.
0148-0227/96/95JB-03446$05.00

well as incompressible solids, have $\sigma = 0.5$. A negative value of σ implies that a cylinder undergoing compression along its axis would contract simultaneously in all directions. Negative values of σ have been observed for certain directions in single crystals [*Svetlov et al.*, 1988].

The relationship between Poisson's ratio and compressional wave velocity (V_p) and shear wave velocity (V_s) for an isotropic medium is given by

$$\sigma = \frac{1}{2}\left[1 - \frac{1}{(V_p/V_s)^2 - 1}\right] . \quad (1)$$

Note that if $\sigma = 0$, $V_p/V_s = \sqrt{2}$ and if $\sigma = 0.5$, $V_p/V_s = \infty$.

A rock is an aggregate of minerals, and at sufficiently high pressures such that porosity is eliminated, a rock's Poisson's ratio is presumably related to the volume percentages of its mineral constituents and the Poisson's ratios of the minerals. Obtaining Poisson's ratios for common rock-forming minerals is complicated, however, by anisotropy. The number of elastic constants of single crystals is symmetry-dependent and, unfortunately, many of the common rock-forming minerals have low symmetries, resulting in large numbers of elastic constants. For example, feldspars, which are the most abundant minerals in the Earth's crust, are either monoclinic or triclinic, with 13 and 21 elastic constants, respectively.

Several methods have been proposed to average the elastic constants of a mineral in order to obtain average velocities which, in turn, can be used to obtain Poisson's ratio from equation (1) for a randomly oriented aggregate of the mineral. *Voigt* [1928] assumed that strain is uniform throughout the mineral and averaged the elastic constants (c_{ij}) over solid angles, whereas *Reuss* [1929] assumed that uniform local stress was operative and averaged the elastic compliances (s_{ij}) over all directions. These averaging techniques yield bulk and shear moduli which, with density, allow the calculation of average compressional and shear velocities. Differences in the Voigt and Reuss averages are appreciable in highly anisotropic minerals. Often the arithmetic mean of the two, the Voigt-Reuss-Hill approximation, is used for calculating average properties of a quasi-isotropic solid. Another commonly used averaging scheme based on assemblages of composite spheres, that of *Hashin and Shtrikman* [1962], provides upper and lower bounds that fall within the Voigt and Reuss averages.

In Table 1, V_p/V_s ratios and Poisson's ratios, calculated from velocities obtained from the averaging schemes discussed above, are given for a variety of rock-forming minerals. The data in Table 1 were obtained from elastic constants measured at room temperature and atmospheric pressure. Many of the measurements were made on crack free gem quality crystals. Pressure and temperature derivatives of the elastic constants have been investigated for only a few of these minerals and will be discussed later in this paper. Several techniques, including the ultrasonic pulse and resonance methods and, more recently, Brillouin scattering, have been utilized to measure the elastic constants [*Schreiber et al.*, 1973]. The quality of the data is variable and likely highest for minerals with orthorhombic and higher symmetries. Chemical analyses were not reported in many of the earlier studies, which include important rock-forming silicates such as the feldspars, hornblende, and several of the pyroxenes of Table 1.

Table 1. Compressional (V_p) and Shear (V_s) Wave Velocity Ratios and Poisson's Ratios for Rock-Forming Minerals

Mineral	Symmetry[a]	Density, (kg/m^3)	V_p/V_s					Poisson's Ratio					Reference
			R	HS$^-$	VRH	HS$^+$	V	R	HS$^-$	VRH	HS$^+$	V	
Framework silicates													
Feldspars													
Microcline[b]	T	2561	1.856	1.857	1.838	1.844	1.822	0.296	0.296	0.290	0.292	0.285	*Ryzhova and Alexandrov* [1965]
Plagioclase(An_9)	T	2610	1.819	1.819	1.817	1.819	1.816	0.283	0.284	0.283	0.283	0.282	*Ryzhova* [1964]
Plagioclase(An_{24})	T	2640	1.840	1.835	1.832	1.831	1.823	0.291	0.289	0.288	0.288	0.285	*Ryzhova* [1964]
Plagioclase(An_{29})	T	2640	1.841	1.835	1.830	1.830	1.820	0.291	0.289	0.287	0.287	0.284	*Ryzhova* [1964]
Plagioclase(An_{53})	T	2680	1.875	1.863	1.858	1.856	1.842	0.301	0.298	0.296	0.295	0.291	*Ryzhova* [1964]
Plagioclase(An_{56})	T	2690	1.872	1.859	1.853	1.851	1.836	0.300	0.296	0.295	0.294	0.289	*Ryzhova* [1964]
Quartz	TR	2649	1.498	1.482	1.477	1.475	1.458	0.098	0.082	0.077	0.074	0.056	*McSkimin et al.* [1965]
Natrolite	O	2250	1.737	1.733	1.733	1.731	1.728	0.252	0.250	0.250	0.249	0.248	*Ryzhova et al.* [1966]
Sheet silicates													
Muscovite	M	2844	1.760	1.740	1.729	1.721	1.704	0.261	0.253	0.249	0.245	0.237	*Vaughan and Guggenheim* [1986]
Biotite	M	3050	2.155	1.948	1.831	1.719	1.656	0.363	0.321	0.288	0.244	0.213	*Alexandrov and Ryzhova* [1961a]
Phlogopite	M	2810	2.177	1.988	1.872	1.769	1.696	0.366	0.331	0.300	0.265	0.234	*Alexandrov and Ryzhova* [1961a]

Table 1. (continued)

Mineral	Symmetry[a]	Density, (kg/m^3)	V_p/V_s R	V_p/V_s HS$^-$	V_p/V_s VRH	V_p/V_s HS$^+$	V_p/V_s V	Poisson's Ratio R	Poisson's Ratio HS$^-$	Poisson's Ratio VRH	Poisson's Ratio HS$^+$	Poisson's Ratio V	Reference
Chain silicates													
Amphibole													
Hornblende	M	3120	1.835	1.832	1.831	1.831	1.828	0.289	0.288	0.287	0.288	0.286	*Alexandrov and Ryzhova* [1961b]
Pyroxenes													
Enstatite	O	3272	1.648	1.648	1.648	1.648	1.649	0.208	0.209	0.209	0.209	0.209	*Duffy and Vaughan* [1988]
Bronzite	O	3380	1.739	1.737	1.737	1.737	1.735	0.253	0.252	0.252	0.252	0.251	*Ryzhova et al.* [1966]
Orthoferrosilite	O	4002	1.807	1.810	1.809	1.810	1.812	0.279	0.280	0.280	0.280	0.281	*Bass and Weidner* [1984]
Diopside	M	3270	1.745	1.755	1.756	1.760	1.767	0.255	0.260	0.260	0.262	0.264	*Levien et al.* [1979]
Jadeite	M	3400	1.743	1.739	1.738	1.737	1.732	0.255	0.253	0.252	0.252	0.250	*Kandelin and Weidner* [1988a]
Hedenbergite	M	3640	1.804	1.809	1.810	1.811	1.815	0.278	0.280	0.280	0.281	0.282	*Kandelin and Weidner* [1988b]
Augite	M	3320	1.717	1.727	1.727	1.731	1.737	0.243	0.248	0.248	0.249	0.252	*Alexandrov et al.* [1964]
Diallage	M	3300	1.650	1.649	1.648	1.648	1.646	0.210	0.209	0.209	0.209	0.208	*Alexandrov et al.* [1964]
Aegirine-augite	M	3420	1.850	1.869	1.869	1.876	1.886	0.294	0.299	0.299	0.302	0.305	*Alexandrov et al.* [1964]
Aegirine	M	3500	1.801	1.800	1.799	1.799	1.797	0.277	0.277	0.276	0.276	0.276	*Alexandrov et al.* [1964]
Orthosilicates and ring silicates													
Olivine group													
Forsterite	O	3224	1.712	1.710	1.710	1.709	1.708	0.241	0.240	0.240	0.240	0.239	*Kumazawa and Anderson* [1969]
Olivine(Fo_{93})	O	3311	1.725	1.724	1.724	1.724	1.722	0.247	0.247	0.246	0.246	0.246	*Kumazawa and Anderson* [1969]
Fayalite(Fe_2SiO_4)	O	4400	2.029	2.014	2.011	2.007	1.994	0.340	0.336	0.336	0.335	0.332	*Sumino* [1979]
Garnet group													
Spessartite-almandine	C	4249	1.784	1.784	1.784	1.784	1.784	0.271	0.271	0.271	0.271	0.271	*Wang and Simmons* [1974]
Almandine	C	4160	1.792	1.792	1.792	1.792	1.792	0.274	0.274	0.274	0.274	0.274	*Soga* [1967]
Grossularite	C	3617	1.725	1.725	1.725	1.725	1.724	0.247	0.247	0.247	0.247	0.247	*Halleck* [1973]
Staurolite	M	3369	1.606	1.618	1.627	1.628	1.646	0.183	0.191	0.196	0.197	0.208	*Alexandrov and Ryzhova* [1961c]
Sillimanite	O	3241	1.791	1.784	1.783	1.781	1.776	0.273	0.271	0.271	0.270	0.268	*Vaughan and Weidner* [1978]
Andalusite	O	3145	1.718	1.723	1.723	1.724	1.728	0.244	0.246	0.246	0.247	0.248	*Vaughan and Weidner* [1978]
Epidote	M	3400	1.778	1.755	1.752	1.746	1.728	0.269	0.260	0.258	0.256	0.248	*Ryzhova et al.* [1966]
Beryl	H	2680	1.756	1.750	1.750	1.749	1.745	0.260	0.258	0.258	0.257	0.255	*Hearmon* [1956]
Tourmaline	TR	3050	1.659	1.659	1.657	1.658	1.656	0.215	0.214	0.214	0.214	0.213	*Hearmon* [1956]
Nonsilicates													
Chromite	C	4450	1.813	1.809	1.809	1.808	1.804	0.281	0.280	0.280	0.280	0.278	*Hearmon* [1956]
Magnetite	C	5180	1.763	1.761	1.761	1.761	1.760	0.263	0.262	0.262	0.262	0.262	*Alexandrov and Ryzhova* [1961c]
Pyrite	C	5013	1.582	1.574	1.572	1.555	1.583	0.167	0.162	0.160	0.147	0.168	*Alexandrov and Ryzhova* [1961d]
Calcite	TR	2712	2.027	1.972	1.944	1.931	1.874	0.339	0.327	0.320	0.317	0.301	*Peselnick and Robie* [1963]
Aragonite	O	2930	1.598	1.595	1.597	1.594	1.595	0.178	0.176	0.177	0.176	0.176	*Hearmon* [1956]

R is Reuss average; HS$^-$, Hashin Shtrikman lower bound; VRH, Voigt Reuss Hill average; HS$^+$, Hashin Shtrikman upper bound; V, Voigt average.
[a] Cubic(C), hexagonal(H), trigonal(TR), orthorhombic(O), monoclinic(M), triclinic(T).
[b] Average of seven samples.

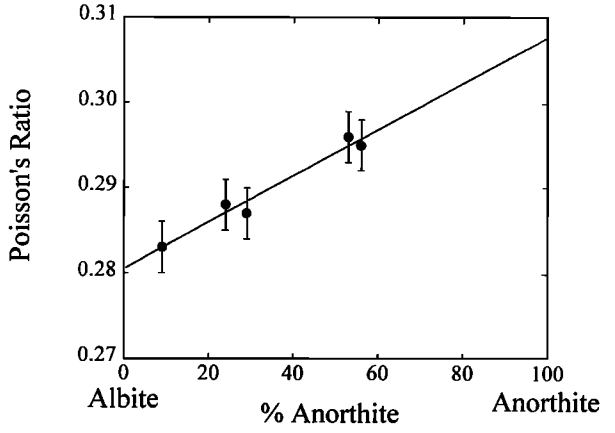

Figure 1. Voigt-Reuss-Hill Poisson's ratios for plagioclase feldspars. Data are from Table 1.

The Voigt and Reuss values of Table 1 differ by only a few percent for many of the minerals, with notable exceptions, including the micas, quartz, and calcite. A comparison of the Voigt-Reuss-Hill averages of Poisson's ratio for the silicate minerals in Table 1 illustrates the extremely low value (0.08) of quartz. The lowest silicate values, except for quartz, are for staurolite (0.20), enstatite (0.21), and diallage (0.21). Poisson's ratios for the feldspars are quite high (0.28 to 0.30), as are those of biotite (0.29), phlogopite (0.30), aegirine-augite (0.30), and fayalite (0.34).

Two chemically related trends in Poisson's ratio are evident from Table 1. First, there is a systematic increase in Poisson's ratio with anorthite content of the plagioclase feldspars (Figure 1). Poisson's ratio of albite increases from 0.279 to a predicted value of 0.314 for anorthite. Plagioclase feldspar is a major constituent of many common crustal igneous and metamorphic rocks, and consideration of the anorthite content is important in understanding Poisson's ratios of these rocks. For example, in plutonic igneous rocks, plagioclase composition changes from albite-rich in granite, through andesine (30% to 50% anorthite) in diorite, to a composition generally in the labradorite range (50% to 70% anorthite) for gabbro. In addition, progressive metamorphism can be accompanied by systematic changes in plagioclase composition. Anorthite-rich plagioclase in basalt breaks down to albite at low metamorphic grades, which increases in anorthite content to andesine in amphibolites and labradorite in mafic granulites. Thus, during progressive metamorphism of mafic rocks, plagioclase should contribute to a gradual increase in Poisson's ratio from zeolite facies assemblages to the granulite facies. The influence of plagioclase composition on rock Poisson's ratios will be discussed in more detail in the following sections.

A second chemical trend in Poisson's ratio is due to Fe-Mg substitution in pyroxenes and olivines (Table 1). The orthopyroxenes (enstatite, bronzite, orthoferrosilite) show an increase in Poisson's ratio from 0.209 in $MgSiO_3$ (enstatite) to 0.280 in $FeSiO_3$ (orthoferrosilite). In the olivine series, Poisson's ratio increases systematically from 0.240 in Mg_2SiO_4 (forsterite) to 0.336 in Fe_2SiO_4 (fayalite). Figure 2 illustrates this latter trend for the three olivine compositions given in Table 1. The vertical error bars on each data point in Figures 1 and 2 are error estimates for Voigt-Reuss-Hill averages.

The systematics of Poisson's ratio and composition are evidently more complex for other silicates. For example, muscovite has a lower Poisson's ratio than Fe-rich biotite; however, phlogopite (a Mg-rich mica) has a higher Poisson's ratio than biotite. A comparison of Poisson's ratios for the two polymorphs of Al_2SiO_5 (sillimanite and andalusite) suggests that Poisson's ratio increases with increasing density for minerals of similar composition. Clearly, additional information is needed on the elastic constants of many rock-forming minerals, especially silicates.

Rock Poisson's Ratios

Rock Poisson's ratios can be calculated from compressional and shear wave velocity measurements (equation (1)). Velocity measurements are most conveniently made using the pulse transmission technique [*Birch*, 1960] in which arrival times of compressional and shear waves are measured and velocities are calculated from sample lengths and travel times. Velocity measurements at elevated hydrostatic pressures are essential because crack porosity in most rocks does not close until pressures of 100 to 200 MPa are reached. Consequently, large discrepancies in Poisson's ratios are observed when values are calculated from velocities obtained at low pressures.

Average velocities, densities, and their standard deviations at pressures to 1 GPa, corrected for change of dimensions under pressure, are presented in Table 2 for a variety of common rock types. The data set summarizes velocity measurements on 1875 cores taken from 678 rock samples. This represents a subset of rocks for which compressional wave velocities were presented by *Christensen and Mooney* [1995]. The rocks have been divided into 29 major groups, details of which are given by Christensen and Mooney. Classification has been kept as simple as possible. For each rock sample, with the exception of a few isotropic granites and basalts, compressional wave velocities were measured in three directions and averaged. Three cores, cut in mutually perpendicular directions, were taken from most samples with core orientations controlled by rock symmetry [*Birch*, 1960; *Christensen*, 1966a; *Christensen and Szymanski*, 1988]. For anisotropic samples, shear wave splitting measurements were obtained for each core and shear wave velocities for each rock

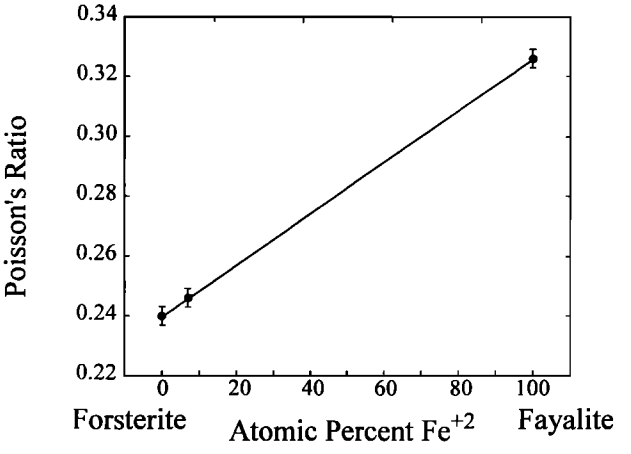

Figure 2. The relationship between Poisson's ratio and chemical composition for the common olivines. Data are from Table 1.

Table 2. V_p and V_s as Function of Pressure

Name Specimens (s) Rocks (r)		ρ, kg/m³	200 MPa		400 MPa		600 MPa		800 MPa		1000 MPa	
			V_p	V_s	V_p	V_s	V_p	V_s	V_p	V_s	V_p	V_s
Andesite (AND)												
s=30	Average	2627	5.533	3.034	5.712	3.097	5.814	3.130	5.885	3.155	5.940	3.177
r=10	S.D.	71	0.260	0.208	0.227	0.207	0.224	0.204	0.226	0.207	0.229	0.248
Basalt (BAS)												
s=252	Average	2882	5.914	3.217	5.992	3.246	6.044	3.264	6.084	3.279	6.118	3.291
r=145	S.D.	139	0.546	0.302	0.544	0.293	0.543	0.291	0.542	0.288	0.542	0.288
Diabase (DIA)												
s=45	Average	2936	6.712	3.729	6.756	3.748	6.782	3.757	6.800	3.762	6.814	3.766
r=15	S.D.	91	0.266	0.170	0.254	0.156	0.249	0.151	0.244	0.144	0.243	0.141
Granite-granodiorite (GRA)												
s=108	Average	2652	6.246	3.669	6.296	3.692	6.327	3.706	6.352	3.717	6.372	3.726
r=38	S.D.	23	0.128	0.116	0.121	0.104	0.121	0.100	0.123	0.096	0.124	0.095
Diorite (DIO)												
s=24	Average	2810	6.497	3.693	6.566	3.717	6.611	3.733	6.646	3.745	6.675	3.756
r=8	S.D.	85	0.161	0.120	0.144	0.110	0.134	0.106	0.120	0.101	0.120	0.099
Gabbro-norite-troctolite (GAB)												
s=174	Average	2968	7.138	3.862	7.200	3.888	7.241	3.905	7.273	3.918	7.299	3.929
r=58	S.D.	69	0.252	0.129	0.255	0.125	0.258	0.124	0.261	0.124	0.263	0.124
Metagraywacke (MGW)												
s=27	Average	2682	5.829	3.406	5.950	3.448	6.028	3.474	6.089	3.495	6.139	3.512
r=9	S.D.	52	0.348	0.291	0.309	0.273	0.283	0.265	0.234	0.253	0.231	0.249
Slate (SLT)												
s=27	Average	2807	6.156	3.301	6.240	3.351	6.297	3.384	6.342	3.410	6.379	3.432
r=9	S.D.	21	0.103	0.106	0.099	0.096	0.094	0.090	0.081	0.081	0.075	0.077
Phyllite, phyllonite (PHY)												
s=57	Average	2738	6.243	3.543	6.305	3.569	6.343	3.585	6.373	3.597	6.398	3.608
r=19	S.D.	46	0.116	0.140	0.093	0.139	0.090	0.140	0.087	0.140	0.086	0.140
Zeolite facies basalt (BZE)												
s=54	Average	2915	6.319	3.413	6.400	3.444	6.454	3.464	6.495	3.480	6.530	3.493
r=18	S.D.	83	0.270	0.152	0.262	0.152	0.259	0.153	0.256	0.155	0.255	0.156
Prehnite-pumpellyite facies basalt (BPP)												
s=36	Average	2835	6.353	3.545	6.436	3.575	6.492	3.595	6.535	3.610	6.571	3.623
r=12	S.D.	108	0.414	0.237	0.370	0.219	0.354	0.214	0.334	0.207	0.326	0.204
Greenschist facies basalt (BGR)												
s=36	Average	2978	6.820	3.883	6.884	3.911	6.925	3.929	6.957	3.943	6.983	3.955
r=12	S.D.	86	0.227	0.131	0.220	0.134	0.221	0.137	0.223	0.141	0.225	0.143
Granite gneiss (GGN)												
s=72	Average	2643	6.010	3.501	6.145	3.553	6.208	3.583	6.245	3.607	6.271	3.627
r=24	S.D.	46	0.184	0.167	0.135	0.143	0.122	0.137	0.107	0.130	0.101	0.128
Biotite (tonalite) gneiss (BGN)												
s=156	Average	2742	6.180	3.552	6.256	3.585	6.302	3.606	6.337	3.622	6.366	3.636
r=52	S.D.	68	0.189	0.166	0.171	0.150	0.166	0.148	0.161	0.141	0.160	0.139
Mica quartz schist (QSC)												
s=87	Average	2824	6.267	3.526	6.370	3.579	6.433	3.610	6.482	3.634	6.523	3.654
r=29	S.D.	122	0.307	0.232	0.310	0.227	0.314	0.228	0.321	0.219	0.324	0.217
Amphibolite (AMP)												
s=78	Average	2996	6.866	3.909	6.939	3.941	6.983	3.959	7.018	3.974	7.046	3.987
r=26	S.D.	85	0.224	0.151	0.199	0.136	0.197	0.133	0.197	0.131	0.197	0.130
Felsic granulite (FGR)												
s=87	Average	2758	6.411	3.608	6.474	3.631	6.514	3.646	6.545	3.657	6.571	3.667
r=29	S.D.	79	0.132	0.134	0.127	0.125	0.127	0.125	0.129	0.126	0.131	0.127
Paragranulite (PGR)												
s=72	Average	2761	6.339	3.590	6.402	3.617	6.441	3.634	6.471	3.647	6.497	3.658
r=14	S.D.	56	0.173	0.129	0.143	0.124	0.138	0.119	0.135	0.116	0.135	0.115
Anorthositic granulite (AGR)												
s=30	Average	2763	6.931	3.736	7.003	3.766	7.049	3.784	7.085	3.798	7.114	3.810
r=10	S.D.	63	0.134	0.105	0.138	0.105	0.140	0.107	0.145	0.110	0.147	0.112
Mafic granulite (MGR)												
s=102	Average	2971	6.839	3.767	6.902	3.799	6.942	3.820	6.973	3.836	7.000	3.849
r=34	S.D.	82	0.182	0.121	0.181	0.115	0.184	0.113	0.190	0.111	0.193	0.111

Table 2. (continued)

Name Specimens (s) Rocks (r)		ρ, kg/m³	200 MPa		400 MPa		600 MPa		800 MPa		1000 MPa	
			V_p	V_s	V_p	V_s	V_p	V_s	V_p	V_s	V_p	V_s
Mafic garnet granulite (GGR)												
s=81	Average	3111	7.110	3.974	7.197	4.007	7.249	4.026	7.290	4.040	7.324	4.052
r=27	S.D.	104	0.184	0.122	0.164	0.108	0.154	0.105	0.154	0.104	0.154	0.104
Mafic eclogite (ECL)												
s=51	Average	3485	8.001	4.481	8.078	4.524	8.127	4.553	8.166	4.575	8.198	4.594
r=17	S.D.	67	0.156	0.145	0.160	0.141	0.156	0.143	0.150	0.150	0.149	0.147
Serpentinite (SER)												
s=30	Average	2566	5.308	2.588	5.421	2.610	5.497	2.625	5.557	2.636	5.607	2.646
r=10	S.D.	50	0.335	0.177	0.308	0.173	0.295	0.170	0.273	0.166	0.263	0.163
Quartzite (QTZ)												
s=24	Average	2652	5.963	4.035	6.012	4.048	6.045	4.052	6.070	4.053	6.091	4.054
r=8	S.D.	8	0.074	0.048	0.076	0.042	0.077	0.041	0.078	0.040	0.079	0.040
Calcite marble (MBL)												
s=21	Average	2721	6.916	3.653	6.944	3.707	6.961	3.743	6.974	3.770	6.985	3.794
r=7	S.D.	12	0.085	0.188	0.080	0.181	0.080	0.180	0.080	0.179	0.081	0.179
Anorthosite (ANO)												
s=45	Average	2730	6.978	3.653	7.035	3.678	7.072	3.694	7.101	3.707	7.124	3.717
r=15	S.D.	38	0.218	0.169	0.205	0.170	0.203	0.171	0.202	0.174	0.203	0.174
Hornblendite (HBL)												
s=6	Average	3248	7.161	4.094	7.222	4.129	7.261	4.144	7.291	4.153	7.317	4.160
r=2	S.D.	1	0.020	0.013	0.010	0.022	0.021	0.029	0.036	0.035	0.041	0.037
Pyroxenite (PYX)												
s=27	Average	3267	7.737	4.444	7.812	4.473	7.863	4.492	7.902	4.506	7.935	4.519
r=9	S.D.	30	0.114	0.179	0.099	0.174	0.097	0.172	0.097	0.170	0.098	0.169
Dunite (DUN)												
s=36	Average	3310	8.299	4.731	8.352	4.759	8.376	4.771	8.390	4.778	8.399	4.783
r=12	S.D.	14	0.091	0.118	0.083	0.116	0.083	0.116	0.084	0.116	0.085	0.116

V_p and V_s are in kilometers per second.

were averaged from the six velocity measurements at a given pressure. Velocity ratios and Poisson's ratios are given in Table 3 at five pressures.

Early measurements of shear wave velocities were often the subject of much uncertainty. Onsets of first arrivals were gradual and shear wave splitting was not investigated, giving rise to shear velocity accuracies of several percent [*Kanamori and Mizutani*, 1965; *Christensen and Shaw*, 1970]. Improved transducers and techniques for velocity measurements [*Christensen*, 1985] have significantly increased both compressional and shear wave velocity accuracies to approximately 1/2%. This is particularly important for calculations of Poisson ratios from velocity measurements.

Rearranging equation (1) gives

$$\sigma = \frac{\eta^2 - 2}{2(\eta^2 - 1)} \tag{2}$$

where $\eta = V_p/V_s$, it follows that

$$\left|\frac{\Delta\sigma}{\sigma}\right| = f(\eta)\left(\left|\frac{\Delta V_p}{V_p}\right| + \left|\frac{\Delta V_s}{V_s}\right|\right) \tag{3}$$

where

$$f(\eta) = \frac{2\eta^2}{(\eta^2 - 1)(\eta^2 - 2)} . \tag{4}$$

A plot of $f(V_p/V_s)$ versus V_p/V_s (Figure 3) shows that larger errors in σ calculated from velocity measurements occur for rocks with low velocity ratios (low Poisson's ratios). The insert in Figure 3 gives $f(V_p/V_s)$ for common rocks with velocity ratios ranging from 1.50 (quartzite) to 2.12 (serpentinite). For an average rock velocity ratio of 1.78 (σ = 0.27), 1/2% errors in V_p and V_s measurements give a maximum error in Poisson's ratio of 2.5% (± 0.005), whereas errors of 2% in both V_p and V_s can result in an error of over 9% (± 0.024) in Poisson's ratio. This is an important consideration in calculations of Poisson's ratios, both from laboratory and field velocities.

Constraints on Crustal Composition

The compilations presented in Tables 1-3 provide several generalizations on the correlation between Poisson's ratio and composition. In this section we examine the roles of pressure, temperature, mineralogy, petrology, and chemistry in determining Poisson's ratios.

Pressure and Temperature Effects

In using Poisson's ratio to place constraints on crustal petrology, it is important to understand how Poisson's ratio varies with pressure and temperature. The compilation in Table 3 provides information on the pressure dependence of Poisson's ratio to pressures equivalent to depths of approxi-

Table 3. V_p/V_s and σ as Function of Pressure

Name Specimens (s) Rocks (r)		200 MPa		400 MPa		600 MPa		800 MP		1000 MPa	
		V_p/V_s	σ	V_p/V_s	σ	V_p/V_s	σ	V_p/V_s	σ	V_p/V_s	σ
Andesite (AND)											
s=30	Average	1.823	0.285	1.844	0.292	1.858	0.296	1.865	0.298	1.870	0.300
r=10	S.D.	0.090	0.030	0.085	0.027	0.085	0.027	0.113	0.032	0.176	0.039
Basalt (BAS)											
s=252	Average	1.838	0.290	1.846	0.292	1.851	0.294	1.856	0.295	1.859	0.296
r=145	S.D.	0.047	0.016	0.046	0.015	0.046	0.015	0.047	0.015	0.048	0.015
Diabase (DIA)											
s=45	Average	1.800	0.277	1.802	0.278	1.805	0.279	1.807	0.279	1.809	0.280
r=15	S.D.	0.049	0.017	0.047	0.016	0.046	0.016	0.045	0.015	0.044	0.015
Granite-granodiorite (GRA)											
s=108	Average	1.702	0.237	1.705	0.238	1.707	0.239	1.709	0.240	1.710	0.240
r=38	S.D.	0.051	0.024	0.046	0.022	0.045	0.021	0.043	0.020	0.043	0.020
Diorite (DIO)											
s=24	Average	1.759	0.261	1.766	0.264	1.771	0.266	1.775	0.267	1.777	0.268
r=8	S.D.	0.024	0.010	0.026	0.011	0.028	0.011	0.031	0.012	0.032	0.012
Gabbro-norite-troctolite (GAB)											
s=174	Average	1.848	0.293	1.852	0.294	1.854	0.295	1.856	0.296	1.858	0.296
r=58	S.D.	0.048	0.015	0.048	0.015	0.050	0.015	0.050	0.015	0.051	0.015
Metagraywacke (MGW)											
s=27	Average	1.711	0.241	1.725	0.247	1.735	0.251	1.742	0.254	1.748	0.257
r=9	S.D.	0.077	0.032	0.076	0.031	0.079	0.031	0.089	0.033	0..96	0.034
Slate (SLT)											
s=27	Average	1.865	0.298	1.862	0.297	1.861	0.297	1.859	0.297	1.858	0.296
r=9	S.D.	0.071	0.021	0.065	0.019	0.062	0.019	0.056	0.017	0.054	0.017
Phyllite, phyllonite (PHY)											
s=57	Average	1.762	0.262	1.766	0.264	1.769	0.265	1.772	0.266	1.774	0.267
r=19	S.D.	0.068	0.026	0.068	0.026	0.069	0.026	0.070	0.026	0.070	0.027
Zeolite facies basalt (BZE)											
s=54	Average	1.851	0.294	1.858	0.296	1.863	0.298	1.866	0.299	1.869	0.300
r=18	S.D.	0.037	0.011	0.037	0.011	0.037	0.011	0.038	0.011	0.038	0.011
Prehnite-pumpellyite facies basalt (BPP)											
s=36	Average	1.792	0.274	1.800	0.277	1.806	0.279	1.810	0.280	1.814	0.282
r=12	S.D.	0.036	0.013	0.036	0.013	0.037	0.013	0.039	0.013	0.040	0.014
Greenschist facies basalt (BGR)											
s=36	Average	1.756	0.260	1.760	0.262	1.763	0.263	1.764	0.263	1.766	0.264
r=12	S.D.	0.028	0.011	0.024	0.009	0.023	0.009	0.023	0.009	0.023	0.009
Granite gneiss (GGN)											
s=72	Average	1.716	0.243	1.730	0.249	1.732	0.250	1.731	0.250	1.729	0.249
r=24	S.D.	0.046	0.021	0.047	0.021	0.048	0.021	0.050	0.022	0.051	0.022
Biotite (tonalite) gneiss (BGN)											
s=156	Average	1.740	0.253	1.745	0.255	1.747	0.257	1.749	0.257	1.751	0.258
r=52	S.D.	0.079	0.034	0.077	0.033	0.077	0.033	0.075	0.032	0.075	0.032
Mica quartz schist (QSC)											
s=87	Average	1.777	0.268	1.780	0.269	1.782	0.270	1.784	0.271	1.785	0.271
r=29	S.D.	0.147	0.054	0.145	0.053	0.146	0.054	0.142	0.051	0.141	0.051
Amphibolite (AMP)											
s=78	Average	1.756	0.260	1.761	0.262	1.764	0.263	1.766	0.264	1.767	0.265
r=26	S.D.	0.041	0.017	0.042	0.017	0.043	0.017	0.044	0.017	0.044	0.017
Felsic granulite (FGR)											
s=87	Average	1.777	0.268	1.783	0.270	1.787	0.272	1.790	0.273	1.792	0.274
r=29	S.D.	0.066	0.025	0.063	0.023	0.064	0.023	0.065	0.023	0.065	0.023
Paragranulite (PGR)											
s=72	Average	1.766	0.264	1.770	0.265	1.772	0.266	1.774	0.267	1.776	0.268
r=14	S.D.	0.064	0.024	0.062	0.023	0.062	0.022	0.061	0.022	0.060	0.022
Anorthositic granulite (AGR)											
s=30	Average	1.855	0.295	1.860	0.297	1.863	0.298	1.865	0.298	1.867	0.299
r=10	S.D.	0.033	0.011	0.030	0.010	0.030	0.010	0.031	0.010	0.032	0.010
Mafic granulite (MGR)											
s=102	Average	1.815	0.282	1.817	0.283	1.817	0.283	1.818	0.283	1.818	0.283
r=34	S.D.	0.041	0.015	0.036	0.013	0.035	0.012	0.036	0.013	0.038	0.013

Table 3. (continued)

Name Specimens (s) Rocks (r)		200 MPa		400 MPa		600 MPa		800 MP		1000 MPa	
		V_p/V_s	σ	V_p/V_s	σ	V_p/V_s	σ	V_p/V_s	σ	V_p/V_s	σ
Mafic garnet granulite (GGR)											
s=81	Average	1.789	0.273	1.796	0.275	1.801	0.277	1.804	0.278	1.807	0.279
r=27	S.D.	0.039	0.014	0.041	0.014	0.043	0.015	0.044	0.016	0.046	0.016
Mafic eclogite (ECL)											
s=51	Average	1.786	0.272	1.785	0.271	1.785	0.271	1.785	0.271	1.785	0.271
r=17	S.D.	0.044	0.017	0.043	0.016	0.044	0.016	0.044	0.016	0.044	0.016
Serpentinite (SER)											
s=30	Average	2.051	0.344	2.077	0.349	2.094	0.352	2.108	0.355	2.119	0.357
r=10	S.D.	0.053	0.011	0.052	0.010	0.053	0.010	0.056	0.010	0.059	0.011
Quartzite (QTZ)											
s=24	Average	1.478	0.077	1.485	0.085	1.492	0.092	1.498	0.098	1.502	0.102
r=8	S.D.	0.027	0.027	0.025	0.024	0.025	0.023	0.024	0.022	0.024	0.022
Calcite marble (MBL)											
s=21	Average	1.893	0.307	1.873	0.301	1.860	0.297	1.850	0.294	1.841	0.291
r=7	S.D.	0.087	0.023	0.083	0.023	0.081	0.024	0.079	0.025	0.078	0.026
Anorthosite (ANO)											
s=45	Average	1.910	0.311	1.913	0.312	1.914	0.312	1.916	0.313	1.917	0.313
r=15	S.D.	0.071	0.018	0.070	0.018	0.070	0.018	0.070	0.018	0.070	0.018
Hornblendite (HBL)											
s=6	Average	1.749	0.257	1.749	0.257	1.752	0.258	1.755	0.260	1.759	0.261
r=2	S.D.	0.004	0.002	0.007	0.003	0.007	0.003	0.006	0.003	0.006	0.002
Pyroxenite (PYX)											
s=27	Average	1.741	0.254	1.747	0.256	1.751	0.258	1.754	0.259	1.756	0.260
r=9	S.D.	0.068	0.029	0.066	0.028	0.065	0.027	0.066	0.027	0.066	0.027
Dunite (DUN)											
s=36	Average	1.754	0.259	1.755	0.260	1.756	0.260	1.756	0.260	1.756	0.260
r=12	S.D.	0.045	0.018	0.044	0.017	0.044	0.017	0.044	0.017	0.044	0.017

mately 35 km (1 GPa) for major rock types. Figure 4 illustrates this for several lithologies. There is a slight, barely significant, increase in Poisson's ratio with increasing pressure. Values at low pressures (below 100 MPa) not shown in Figure 4 show considerable scatter due to porosity.

Laboratory data on the influence of temperature on Poisson's ratio are rather limited. In Figure 5, Poisson's ratios calculated from Voigt-Reuss-Hill aggregate velocities are shown versus temperature for quartz and several minerals

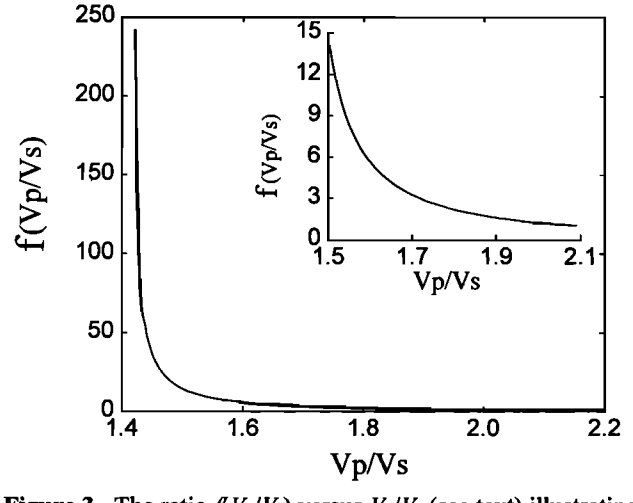

Figure 3. The ratio $f(V_p/V_s)$ versus V_p/V_s (see text) illustrating relative errors in Poisson's ratios calculated from velocities.

with olivine structures. Although it would be desirable to have more complete information for other silicates, the olivine data are of high quality and show that Poisson's ratio does not vary appreciably with temperature. At temperatures from 0°C to 400°C, Poisson's ratio decreases by 0.2% for Co_2SiO_4 olivine and increases by 0.8% to 1.1% for the other varieties of olivine. Similar calculations of Poisson's ratio from velocity measurements in rocks at high temperatures also show little change with temperature (Figure 6). From 20°C to 700°C, the average increase in Poisson's ratio for the eight rocks in Figure 6 is 1.0%, which is within the experimental error. Poisson's ratio of quartzite shows a significant decrease in the 200°C to 500°C temperature range associated with the quartz α-β phase transition [*Kern*, 1982]. Quartz-bearing granite and granulite, however, show only slight decreases in Poisson's ratio with increasing temperature up to 500°C. Since both pressure and temperature dependencies appear to be small for most rocks, laboratory determinations of Poisson's ratios should be directly applicable over a wide range of crustal depths.

Mineral and Rock Comparisons

We can make comparisons for the monomineralic rock averages included in Table 3 with theoretical Poisson's ratios calculated from single crystal elastic constants. These comparisons are summarized in Table 4. The agreement is remarkably good, considering the theoretical uncertainties in calculating average velocities from single-crystal elastic constants, the low symmetries of the single crystals, and the

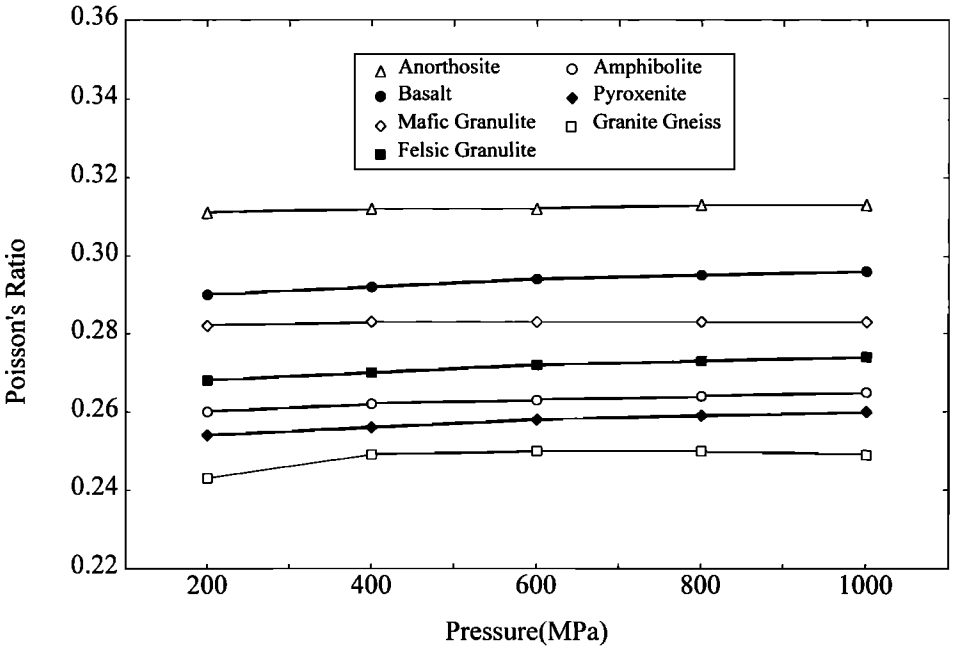

Figure 4. Poisson's ratios versus pressure for selected lithologies of Table 3.

compositional variability inherent to several of the minerals, in particular, plagioclase, amphibole, and pyroxene. Part of the differences in Table 4 is likely due to the presence of accessory minerals in many of the rocks. Petrographic examination and chemical analyses of the quartzites show the presence of traces of feldspar which would slightly increase Poisson's ratio. The average plagioclase composition of the anorthosites is An_{60}, slightly higher than the single-crystal value used for comparison in Table 4. The largest discrepancy is for hornblende, which may be due to differences in chemistry of the mineral and rock samples. Chemistry for the single-crystal hornblende was not reported by *Alexandrov and Ryzhova* [1961b]. Olivine compositions of the dunites are similar to those of the single crystal (Fo_{93}); however, the rocks usually contain a few percent chromite and, for some samples, a trace of serpentine, both of which slightly increase Poisson's ratio. It is concluded that given the constituent mineralogy of a rock, single-crystal data can be used to estimate the expected rock value of Poisson's ratio.

Rock Variability

For the rock types of Table 2, average compressional wave velocities at 600 MPa are plotted versus shear wave velocities in Figure 7. Standard deviations are given in Table 2. Also shown in Figure 7 are lines of constant Poisson's ratios. Of

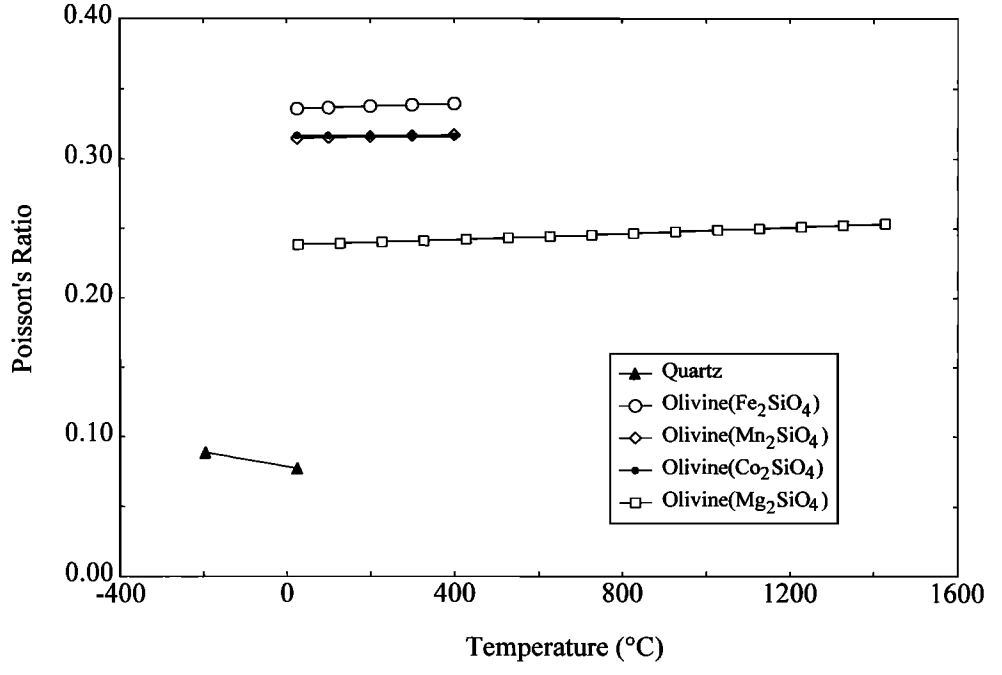

Figure 5. The effect of temperature on Poisson's ratio from single-crystal studies. Data are from *McSkimin et al.* [1965], *Isaak et al.* [1989], and *Sumino* [1979].

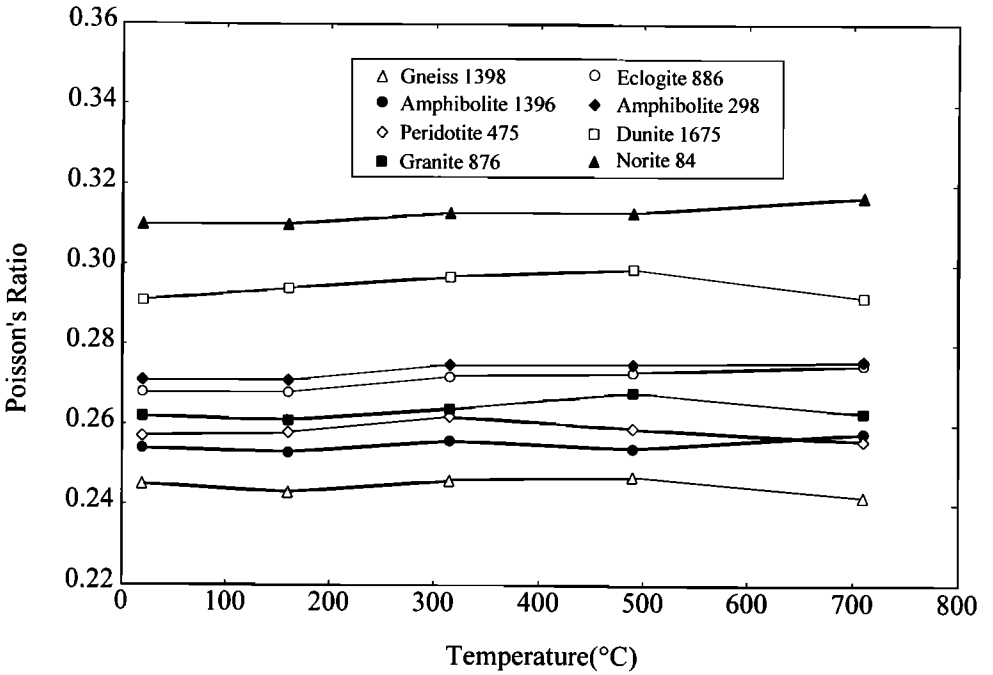

Figure 6. Poisson's ratio versus temperature for rocks at 600 MPa confining pressure [*Kern and Richter*, 1981].

the 29 lithologies, only four have average Poisson's ratios that fall outside the 0.25 to 0.30 range. Two of these, quartzite (QTZ) and granite-granodiorite (GRA), have low Poisson's ratios of 0.092 and 0.239, respectively. Anorthosite (0.312) and serpentinite (0.352) have relatively high values. The average Poisson's ratio for all rock types is 0.27.

Plotting Poisson's ratio versus compressional wave velocity provides a slightly different perspective on the variations of Poisson's ratio for common lithologies (Figure 8). The diagram shows a triangular distribution, which bounds most common rock values: first, quartzite (QTZ) with low velocity and low Poisson's ratio; second, dunite (DUN) with high velocity and intermediate Poisson's ratio; and third, serpentinite (SER) with low velocity and high Poisson's ratio. Another important rock type in this diagram is anorthosite (ANO) with an intermediate velocity, but a high Poisson's ratio. The granite-granodiorite and granitic gneiss fall, as expected, between anorthosite and quartzite, but with Poisson's ratios closer to anorthosite, reflecting the relatively high feldspar-quartz ratios of these rocks. Note that the Poisson's ratio of microcline given in Table 1 is similar to that of intermediate composition plagioclase; however, microcline has a lower compressional wave velocity.

As shown in Figure 8, several rock types with similar compressional wave velocities have quite different Poisson's ratios. For example, average velocities at 600 MPa of slate (SLT), phyllite (PHY) and granite-granodiorite (GRA) are all approximately 6.3 km/s; but average Poisson's ratios for slate, phyllite, and granite-granodiorite are 0.30, 0.265, and 0.24, respectively. Also, amphibolite (AMP), mafic granulite (MGR), and anorthosite (ANO) have similar velocities of approximately 7.0 km/s at 600 MPa. Average Poisson's ratio, however, is relatively low for amphibolite (0.26), intermediate for mafic granulite (0.28), and high for anorthosite (0.31).

A plot of shear wave velocities at 600 MPa versus Poisson's ratios is shown in Figure 9. Important differences between Figures 8 and 9 originate from the high shear wave velocity of quartz, which affects the relative positions of quartz bearing rocks (e.g., granite-granodiorite (GRA) and granitic gneiss (GGN)). Note the high shear wave velocity of quartzite (4.05 km/s), which is greater than that of mafic rocks, including gabbro (GAB), garnet granulite (GGR), and amphibolite (AMP).

Figure 10 illustrates the relation between Poisson's ratio and density. There are many similarities between Figures 8 and 10. Notable differences, however, include the positions of anorthosite (ANO), with its relatively high compressional wave velocity and low density, and eclogite (ECL). Eclogite has the highest density of the data set but not the highest velocity. In the following sections, we examine in more detail variations in Poisson's ratios for igneous rocks and the influence of metamorphic grade on Poisson's ratio.

Table 4. Comparisons of Poisson's Ratios of Single Crystals With Monomineralic Rocks

Mineral	Reuss Average	Voigt Average	Rock	200 MPa	1000 MPa
Quartz	0.098	0.056	quartzite	0.077	0.102
Calcite	0.339	0.301	marble	0.307	0.291
Plagioclase (An_{53})	0.301	0.291	anorthosite	0.311	0.313
Hornblende	0.289	0.286	hornblendite	0.257	0.261
Bronzite	0.253	0.252	pyroxenite	0.254	0.260
Olivine (FO_{93})	0.247	0.246	dunite	0.259	0.260

Igneous Rocks

Poisson's ratios of volcanic rocks are highly variable. This is due to many factors that also produce wide ranges in velocities for these rocks. Alteration is common and many of the alteration products have quite different elastic properties

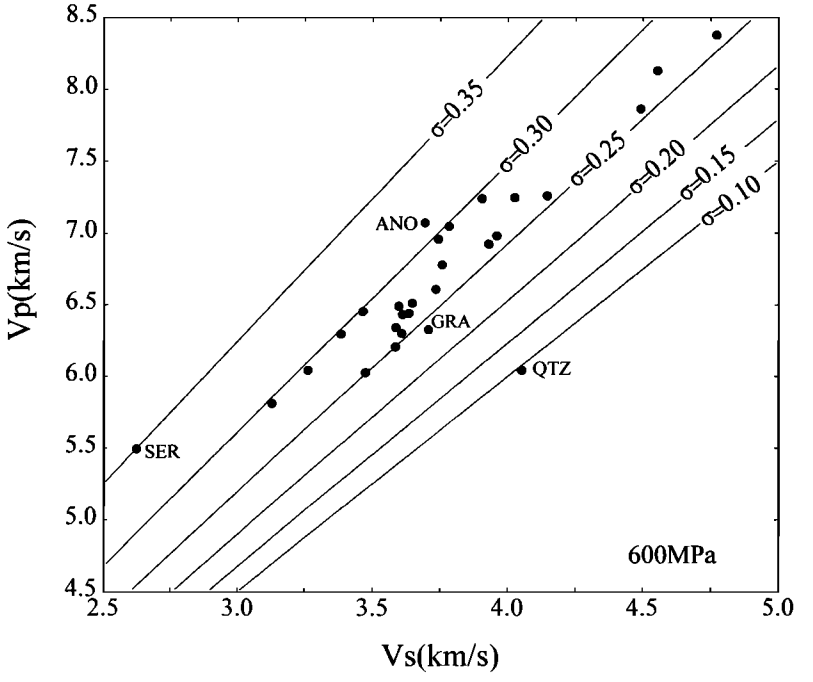

Figure 7. Compressional wave velocities (V_p) versus shear wave velocities (V_s) at 600 MPa for the rock types of Table 2. Four lithologies (serpentinite (SER), anorthosite (ANO), granite-granodiorite (GRA), and quartzite (QTZ)) fall outside the area bounded by Poisson's ratios (σ) between 0.25 and 0.30.

than the parent rocks. Porosity is usually high in volcanic rocks and a significant proportion of porosity is often in the form of small vesicles, which do not close with applied hydro-static pressure [*Birch*, 1961]. Glass is also a common constituent of many volcanic rocks.

There is a clear trend relating Poisson's ratio with composition for common plutonic igneous rocks. In Figure 8, relatively low Poisson's ratios of granitic rocks (~ 0.24) increase to 0.27 as the mineralogy changes to that of diorite (DIO). The transition between diorite and gabbro (GAB) is accompanied by a further increase in Poisson's ratio to 0.295. The low value of granite is in agreement with mineral Poisson's ratios, as discussed earlier, and related primarily to the significant quartz content of granites. The transition from granite to gabbro is accompanied by (1) decreasing modal quartz and (2) an increase in the anorthite content of plagioclase feldspar, both of which increase Poisson's ratio.

Many mafic and ultramafic igneous intrusions contain gabbro and peridotite or dunite which have originated from magmatic differentiation. A gradual change from gabbro to olivine-rich gabbro and dunite lowers the Poisson's ratio to approximately 0.26 (Figure 8) while increasing compressional

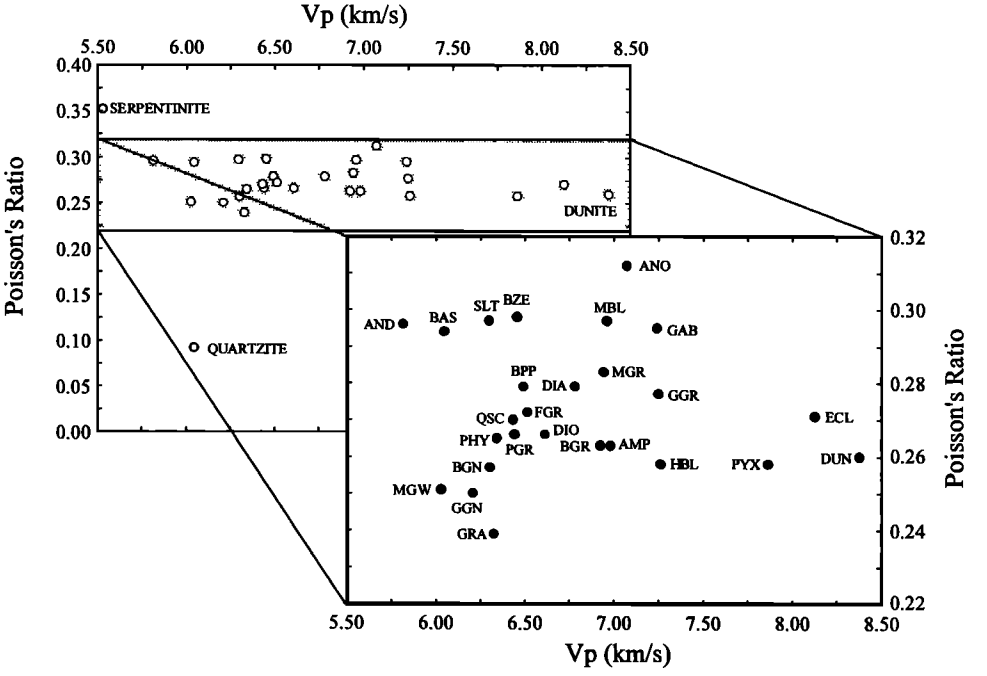

Figure 8. Poisson's ratio versus compressional wave velocity (V_p) at 600 MPa. Rock abbreviations are given in Tables 2 and 3.

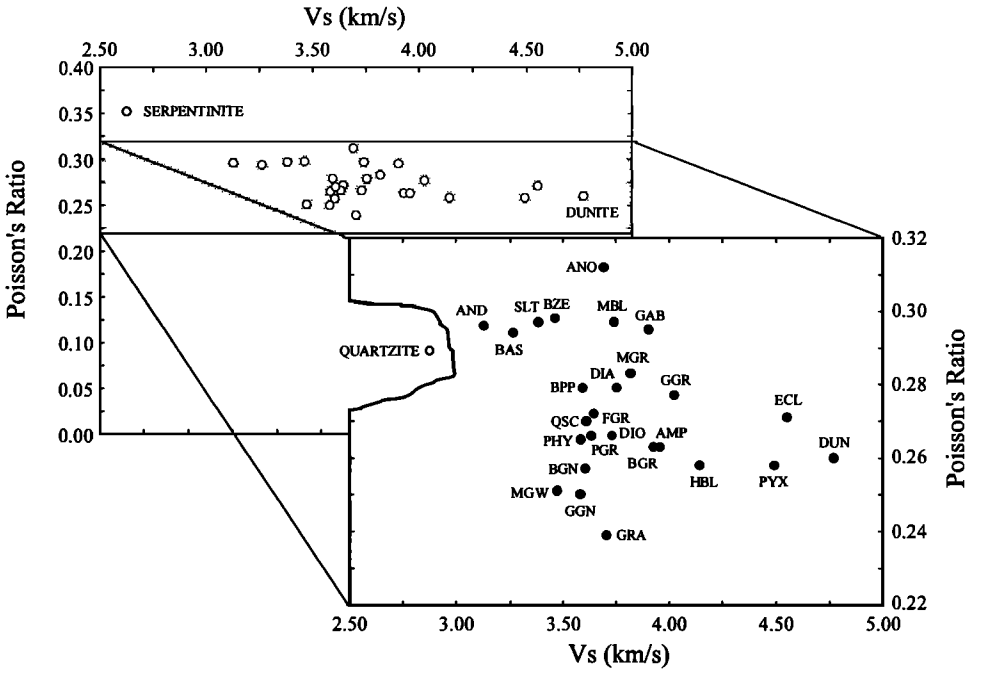

Figure 9. Poisson's ratio versus shear wave velocity (V_s) at 600 MPa. Rock abbreviations are given in Tables 2 and 3.

wave velocity to 8.4 km/s. This decrease in σ is due primarily to decreasing amounts of plagioclase feldspar and increasing olivine content. Thus mineralogical considerations can, in a qualitative manner, account for the Poisson's ratios observed for the plutonic igneous rocks.

Calculated velocities and Poisson's ratios from single crystal elastic constants, based on a relatively simple classification scheme for igneous rocks, are shown in Figure 11. The calculations, using the time-average technique of *Birch* [1961], are based on the mineral volume percentages shown in Figure 11 and the atmospheric pressure Voigt-Reuss-Hill single crystal averages of Table 1. Although less reliable than measured Poisson's ratios, because of theoretical uncertainties and limited silicate mineral elastic constant data, the calculated values show a trend similar to that discussed above. Poisson's ratios increase as composition changes from granite to gabbro and then decrease as the rocks become ultramafic in composition.

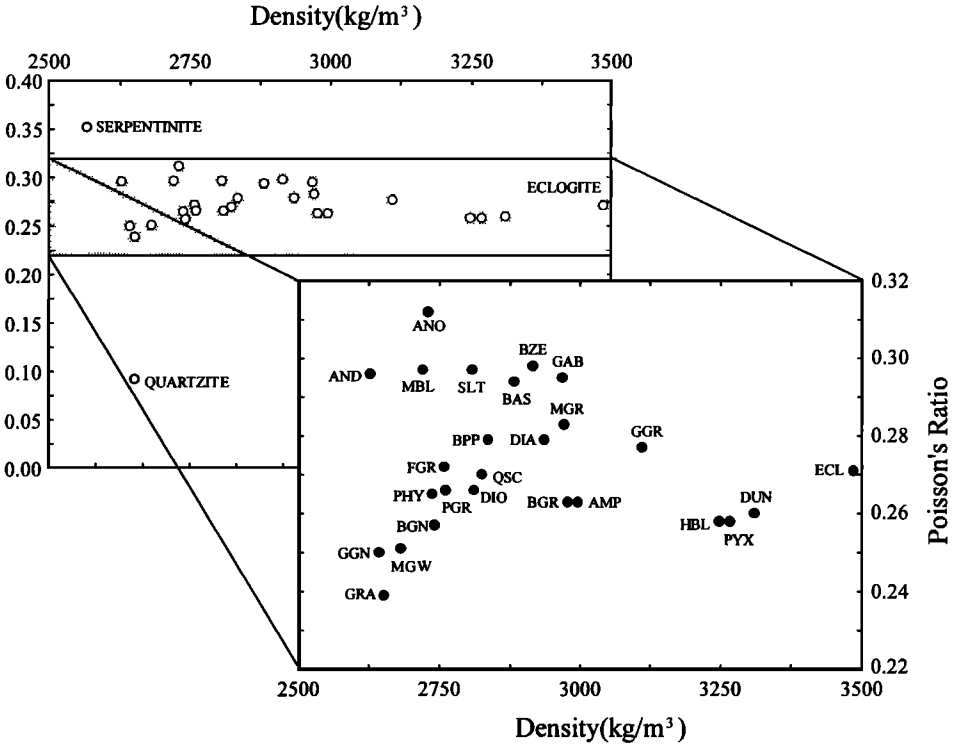

Figure 10. Average densities versus average Poisson's ratios at 600 MPa. See Tables 2 and 3 for rock abbreviations.

Metamorphic Rocks

Metamorphism is an important crustal process, often producing major changes in mineralogy and physical properties. For many rocks these changes are quite complex and sensitive not only to P-T conditions but also to bulk rock chemistry and crustal fluids [e.g., *Yardley*, 1989]. At present, a comprehensive discussion of Poisson's ratios for metamorphic assemblages is difficult due to the limited information on the elastic properties of several important metamorphic minerals. Based on the data in Table 3, however, it is possible to make some preliminary observations on how Poisson's ratio may aid in the interpretation of seismic data from metamorphic crustal regions. The following discussion will be limited to relations between Poisson's ratio and lithology for relatively common metamorphic assemblages.

A simple metamorphic reaction that has importance in oceanic crustal studies is the serpentinization of peridotite [*Hess*, 1962; *Christensen*, 1972]. Changes in elastic properties with serpentinization were well documented several years ago by compressional wave velocity studies of *Birch* [1960, 1961] and shear wave velocity and Poisson's ratio studies of *Christensen* [1966b]. As dunite ($\sigma = 0.25$) is hydrated to serpentinite, there is a progressive change in Poisson's ratio to 0.36 (Table 3 and Figure 8). Partially serpentinized dunites and peridotites have Poisson's ratios that fall between these limiting values and establish a well-defined relationship between Poisson's ratio, percent serpentinization, and density [*Christensen*, 1966b].

It is generally agreed that major portions of the oceanic crust and the lower continental crust contain rocks of mafic composition [*Swift and Stephen*, 1993; *Christensen and Mooney*, 1995]. Metamorphism has been shown to be an important process in the sheeted dike section of the oceanic crust [e.g., *Detrick et al.*, 1994] and in mafic portions of exposed sections of middle to lower crustal rocks [e.g., *Percival et al.*, 1992]. Average Poisson's ratios for a variety of mafic rocks in Table 3 show major changes with increasing metamorphic grade. Initially high Poisson's ratios of low-grade mafic rocks (~ 0.29) decrease significantly to 0.26 for greenschist and amphibolite facies rocks. The transition to the granulite facies is accompanied by an increase in Poisson's ratio to 0.28 followed by a slight decrease to 0.27 as eclogite facies assemblages become stable.

The path of Poisson's ratio outlined above is related to many complex mineral reactions, the most important of which for seismic properties involve changes in the abundances and composition of plagioclase feldspar. Recalling that Poisson's ratio increases with anorthite content and is relatively high for plagioclase (Table 1 and Figure 1), the initial decrease in Poisson's ratio in the low grade mafic rocks originates in part from the breakdown of Ca-rich plagioclase of basalt to Na-rich plagioclase in the prehnite-pumpellyite and greenschist facies assemblages. Plagioclase in the amphibolites is still relatively Na-rich (andesine) and comprises only about 30% of the rock by volume. Progressive metamorphism of amphibolite to mafic granulite is accompanied by increases in the anorthite content of the feldspar and the amount of feldspar, both of which increase Poisson's ratio. The amount of plagioclase as well as the anorthite content decreases in the transition from mafic granulite to eclogite, thereby decreasing the Poisson's ratio. Garnet with a Poisson's ratio of approximately 0.27 (Table 1) becomes abundant in eclogite.

The mafic granulite-eclogite transformation is considered

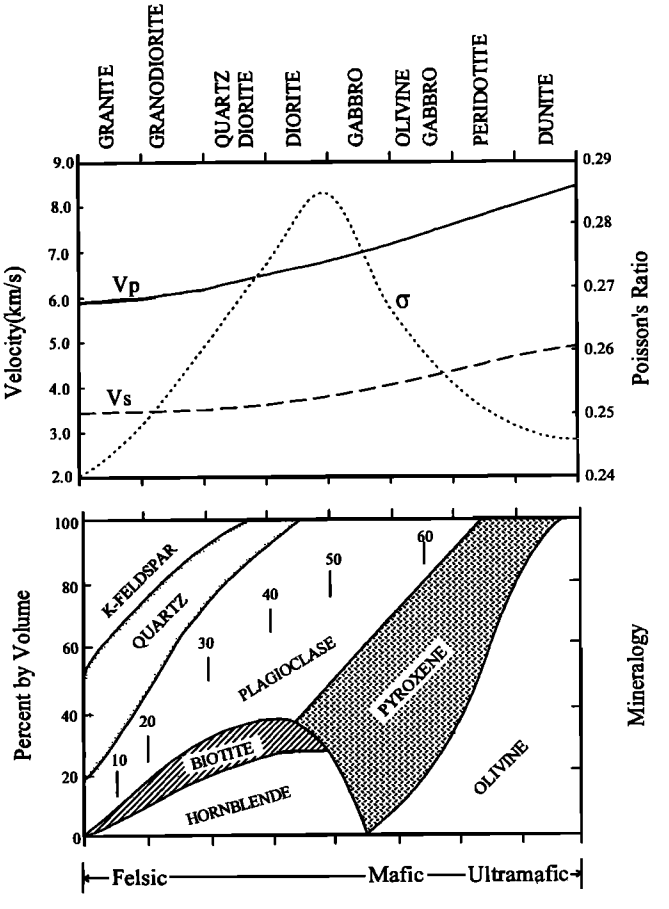

Figure 11. Variations in compressional wave velocity (V_p), shear wave velocity (V_s), and Poisson's ratio (σ) with mineral composition [*Berry and Mason*, 1959] for common igneous rock types. Anorthite content of plagioclase feldspar is shown within the plagioclase field.

to be important in some continental regions as an explanation for the increase in seismic velocities at the Mohorovicic discontinuity [*Griffin and O'Reilly*, 1987]. The changes in mineralogy accompanying this phase change for a quartz tholeiite are shown in Figure 12. Velocities and Poisson's ratios calculated from the atmospheric pressure single-crystal data of Table 1 show significant increases in velocities and a drop in Poisson's ratio with increasing metamorphic grade (Figure 12). Note that compressional wave velocities and Poisson's ratios calculated for eclogite in Figure 12 are significantly lower than eclogite values in Tables 2 and 3. The calculated seismic properties are for eclogite with a much higher quartz content than the average eclogite of Tables 2 and 3.

Poisson's ratio changes associated with progressive metamorphism of pelitic rocks appear to be relatively simple, compared to the above example for mafic rocks. The high Poisson's ratios of slates (0.30) are likely related to the abundance of clay minerals. With the development of mica, Poisson's ratios decrease to 0.27 in phyllite and mica quartz schist and remain constant with further increases in metamorphic grade to paragranulite ($\sigma = 0.27$, Table 3).

Mineralogies and seismic properties of various metabasic rocks and pelitic rocks are summarized in Table 5 for several metamorphic facies. The critical mineral assemblages of each facies [*Yardley*, 1989] are in order of increasing metamorphic grade. Average velocities and Poisson's ratios are from

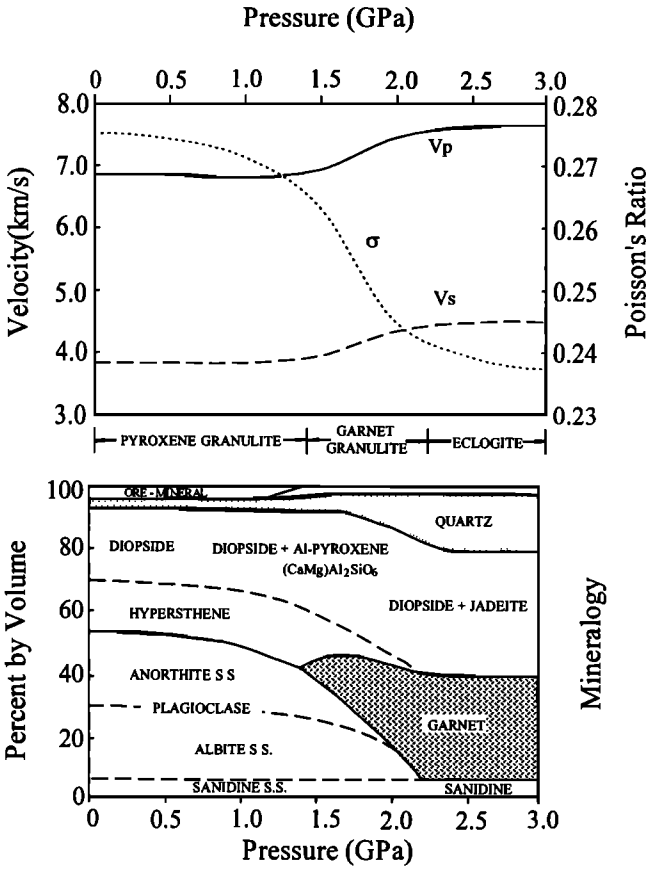

Figure 12. Changes in mineralogy associated with the transition from pyroxene granulite to quartz eclogite for a quartz tholeiite [*Ringwood and Green*, 1966]. The accompanying changes in velocities and Poisson's ratio have been calculated from the Voigt-Reuss-Hill mineral velocities of Table 1.

Tables 2 and 3. The eclogite facies data were obtained by extrapolation to 1.5 Gpa.

The above discussion assumes that rocks are isotropic to seismic wave propagation. Anisotropy is generally low in igneous rocks and in high-grade metamorphic rocks of the granulite facies [*Christensen and Fountain*, 1975; *Christensen and Mooney*, 1995]. Furthermore, no conclusive measurements of lower crustal anisotropy have been reported [*Holbrook et al.*, 1992]. Many low- and intermediate-grade metamorphic rocks are, however, highly anisotropic due to preferred mineral orientations [e.g., *Birch*, 1960], and crustal anisotropy has been observed in upper crustal regions where low- to medium-grade anisotropic rocks are exposed on the surface [e.g., *Brocher and Christensen*, 1990]. Future detailed studies of compressional and shear wave anisotropies in similar crustal regions will be of key importance, since many propagation directions will yield two velocity ratios to provide constraints on composition.

Silica Content

The low Poisson's ratio for quartz is primarily responsible for the relatively low Poisson's ratios of granitic rocks [*Birch*, 1961]. This observation has been the focus of several papers dealing with crustal composition [e.g., *Christensen and Fountain*, 1975; *Holbrook et al.*, 1988; *Johnson and Hartman*, 1991; *Holbrook et al.*, 1992; *White et al.*, 1992]. Often correlations of Poisson's ratio with quartz content are related interchangeably with silica content [e.g., *Tarkov and Vavakin*, 1982; *Clarke and Silver*, 1993]. For most rocks, quartz content is a function of bulk chemistry, in particular silica content; however, some exceptions are notable. For example, cristobalite and/or tridymite, rather than quartz, are abundant in many siliceous volcanic rocks. Rhyolites often have high Poisson's ratios even though their chemistries are practically identical to granites with low Poisson's ratios [*Christensen*, 1982].

The correlation between Poisson's ratio and silica content is illustrated in Figure 13, where average silica contents determined from bulk chemical analyses of the rocks of Table 3 have been plotted versus Poisson's ratio at 600 MPa. All lithologies of Table 3 have been included in the figure, except marble and the volcanic rocks. Two regions are important in this diagram. First, rocks with 55% to 75% SiO_2 show a linear increase in Poisson's ratio with decreasing silica content. A least squares linear fit, percent SiO_2 = 139.0 - 276.0 σ, has been fitted to these rocks at 600 MPa. The coefficient of determination (r^2) is 0.93 for this subset. This solution is shown as the solid line in Figure 13. Also shown is a curved line fit, percent SiO_2 = 100.9 + 496.9σ^2, which includes quartzite as a data set (r^2 = 0.99).

A second region in Figure 13, with silica contents of 40% to 55%, shows much scatter. Note the relatively high Poisson's ratios of anorthosite (ANO) and the low Poisson's ratios of hornblendite (HBL), dunite (DUN), and pyroxenite (PYX). To a first approximation the correlation of Poisson's ratio with silica content holds remarkably well over the range of 55% to 75% SiO_2. Because several mafic lithologies, as well as ultramafic hornblendite and dunite, have relatively low Poisson's ratios, there is no simple correlation between Poisson's ratio and felsic and mafic compositions, as is generally assumed [e.g., *Boland and Ellis*, 1991; *Ward and Warner*, 1991].

Plots of compressional and shear wave velocities versus weight percent SiO_2 show a similar scattering to that of Figure 13 for rocks with SiO_2 contents below 55%. For rocks with SiO_2 contents above 55%, compressional wave velocities decrease and shear wave velocities increase with increasing percentages of SiO_2.

Average Crustal Poisson's Ratios

A variety of techniques has been recently used to estimate average crustal Poisson's ratios ($\bar{\sigma}_c$). *Braile et al.* [1989] combined average crustal shear wave velocities (V_s) derived from surface wave dispersion experiments with average crustal compressional wave velocities (V_p) obtained by interpolating from a crustal V_p contour map of North America to obtain 64 values of $\bar{\sigma}_c$. The average Poisson's ratio for these 64 stations is 0.258 ± 0.034. In their summary of worldwide crustal seismic properties, *Holbrook et al.* [1992] compiled 11 values of $\bar{\sigma}_c$ from wide-angle P and S wave studies. These stations, which were geographically restricted to shields, rifts, and Paleozoic crust, have $\bar{\sigma}_c$ ranging from 0.24 to 0.29.

The use of teleseismic data to obtain relatively accurate values of $\bar{\sigma}_c$ on a global scale shows much promise. Using boundary interaction phases in broadband teleseismic waveforms, *Clarke and Silver* [1993] reported a range of $\bar{\sigma}_c$ from 0.22 to 0.315 for six North American stations. *Zandt and Ammon* [1995] have obtained 76 new estimates of $\bar{\sigma}_c$ using teleseismic converted S waves at the Moho (Ps) and P wave

Table 5. Mineral Assemblages, Average Compressional Wave Velocities (V_p), Average Shear Wave Velocities (V_s), and Average Poisson's Ratios (σ) of the Major Metamorphic Facies

	Metabasic Rocks		Pelitic Rocks	
Facies	Mineralogy	Seismic Properties	Mineralogy	Seismic Properties
Zeolite	laumonite (most typical), analcite, heulandite, wairakite. Incompletely reacted relics widespread	V_p = 6.32 km/s V_s = 3.41 km/s σ = 0.294 p = 0.2 GPa	mixed-layer clays	V_p = 6.16 km/s V_s = 3.30 km/s σ = 0.298 p = 0.2 GPa
Prehnite-pumpellyite	prehnite + pumpellyite ± chlorite ± albite ± epidote (lower temperature zone) pumpellyite + actinolite (higher temperature zone) lawsonite + albite (higher pressure zone)	V_p = 6.39 km/s V_s = 3.56 km/s σ = 0.275 p = 0.3 GPa	illite/muscovite + chlorite + albite + quartz stilpnomelane, pyrophyllite	V_p = 6.20 km/s V_s = 3.33 km/s σ = 0.297 p = 0.3 GPa
Greenschist	actinolite + epidote ± albite ± chlorite ± stilpnomelane (lower temperature zone) hornblende ± actinoline + albite + chlorite + epidote ± garnet (higher temperature zone)	V_p = 6.90 km/s V_s = 3.92 km/s σ = 0.262 p = 0.5 GPa	chlorite + muscovite + albite (lowest temperature zone) chlorite + muscovite + biotite + albite garnet + chlorite + muscovite + biotite + albite (highest temperature zone) chloritoid, paragonite + muscovite + albite	V_p = 6.32 km/s V_s = 3.57 km/s σ = 0.266 p = 0.5 GPa
Amphibolite	hornblende + plagioclase ± epidote ± garnet	V_p = 6.98 km/s V_s = 3.96 km/s σ = 0.263 p = 0.6 GPa	staurolite, kyanite or sillimanite + muscovite (lower temperature zone) sillimanite + K-feldspar ± muscovite + cordierite or garnet sillimanite + garnet + cordierite, no K-feldspar (higher temperature zone)	V_p = 6.43 km/s V_s = 3.61 km/s σ = 0.270 p = 0.6 GPa
Granulite	orthopyroxene + clinopyroxene + plagioclase ± olivine ± hornblende (low pressure) garnet + clinopyroxene + orthopyroxene + plagioclase ± hornblende (medium pressure) garnet + clinopyroxene + quartz + plagioclase ± hornblende (high pressure)	V_p = 7.29 km/s V_s = 4.04 km/s σ = 0.278 p = 0.8 GPa	cordierite + garnet + K-feldspar + sillimanite (moderate pressure) kyanite + K-feldspar (high pressure) hypersthene, sapphirine + quartz (high temperature)	V_p = 6.47 km/s V_s = 3.65 km/s σ = 0.268 p = 0.8 GPa
Eclogite	omphacite + garnet, no plagioclase, no lawsonite	V_p = 8.27 km/s V_s = 4.63 km/s σ = 0.271 p = 1.5 GPa	phengite + chlorite or talc + garnet, no biotite Mg-chloritoid, carpholite	V_p = 6.76 km/s V_s = 3.77 km/s σ = 0.275 p = 1.5 GPa

Mineral assemblages are from *Yardley* [1989].

multiples within the crust (*PpPms*). They find that Precambrian shields have the highest $\bar{\sigma}_c$, averaging 0.29 ± 0.02, whereas Mesozoic/Cenozoic orogenic belts have the lowest values, averaging 0.25 ± 0.04. Their volume weighted average $\bar{\sigma}_c$ for the continental crust is 0.27 ± 0.03.

Field measurements of $\bar{\sigma}_c$ can, in a limited number of cases, be compared with average crustal Poisson's ratios obtained from laboratory studies of crustal cross sections. Unfortunately, most cross sections recognized to date are incomplete, often missing critical lowermost crustal rocks [e.g., *Percival et al.*, 1992] and thus lacking control on crustal thicknesses and average crustal properties. A few surface exposures of oceanic crustal sections are complete [e.g., *Coleman*, 1977]. The Kohistan section in northern Pakistan also records a nearly continuous exposure of an accreted arc terrane. For these sections, velocity profiles have been constructed in detail from compressional and shear wave velocity measurements on samples collected from known stratigraphic levels [*Salisbury and Christensen*, 1978; *Christensen and Salisbury*, 1982; *Christensen and Smewing*, 1981; *Miller and Christensen*, 1994]. Mean crustal velocities corrected for temperature and mean Poisson's ratios are summarized in Table 6 for these sections.

In oceanic crust, the relatively high average Poisson's ratios originate from the high Poisson's ratios of the major lithologies constituting the crust, basalt, diabase, and gabbro (Table 3) and are in reasonable agreement with a 0.32 Poisson's ratio measured by *Bratt and Solomon* [1984] using converted arrivals recorded by ocean bottom seismometers near the East Pacific Rise at 11°N. The oceanic averages of Table 6 do not include a sediment layer. When present, marine sediments will likely increase $\bar{\sigma}_c$ because of their high Poisson's ratios [e.g., *Hamilton*, 1976]. Serpentine diapers within the crust can also contribute to high values of $\bar{\sigma}_c$.

The average crustal compressional wave velocity of *Zandt*

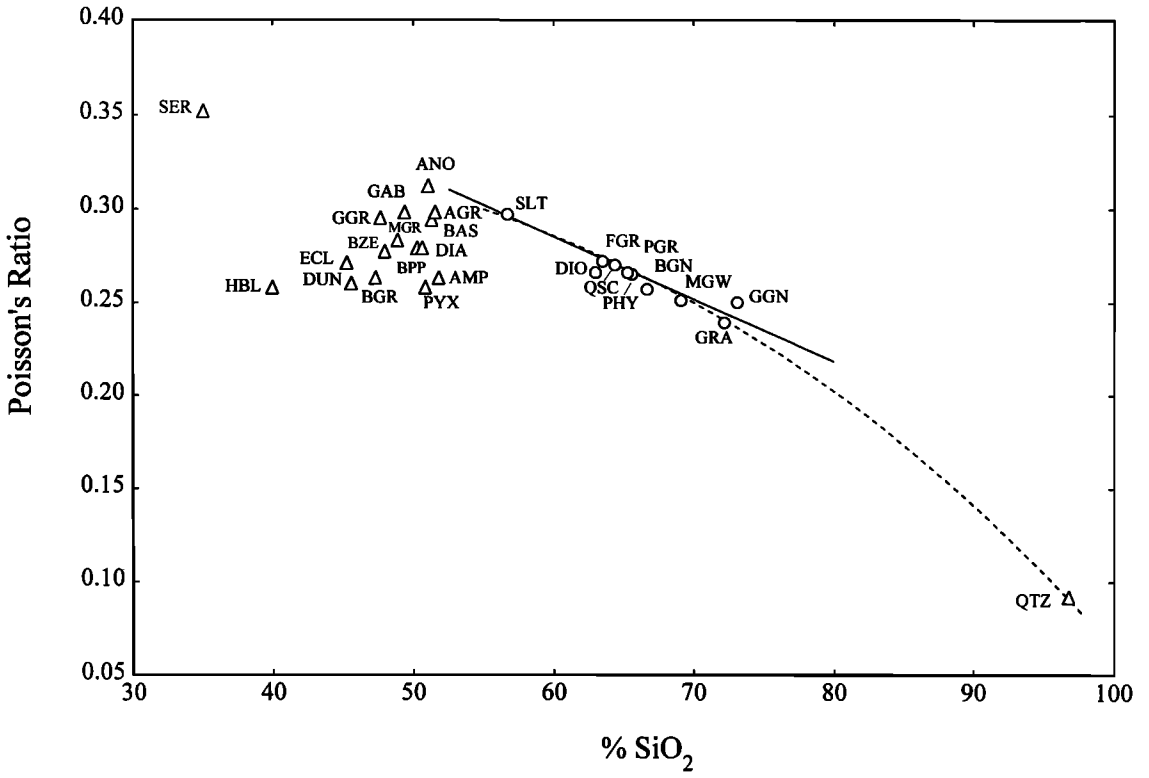

Figure 13. Average Poisson's ratios for common rock types versus their average SiO_2 contents. Rock abbreviations are given in Table 3. The linear solution (see text) is for lithologies with SiO_2 contents between 55 and 75 wt %. The nonlinear solution (see text) includes quartzite (QTZ).

and Ammon [1995] for island arcs is 6.75 km/s, in good agreement with that of the Kohistan arc (Table 6). Their $\bar{\sigma}_c$ of 0.31 ± 0.05 is considerably higher than the 0.27 of *Miller and Christensen* [1994]; however, the Kohistan value falls within one standard deviation of the teleseismic observations.

Estimates of average continental crustal velocities and an average continental crustal Poisson's ratio are also presented in Table 6, based on the recent crustal petrologic model of *Christensen and Mooney* [1995]. In this study an average continental crustal compressional wave velocity-depth profile, derived from a worldwide compilation of 560 seismic studies, was compared with laboratory compressional wave velocity measurements of major continental rock types. A crustal petrologic model was constructed consistent with common lithologies found in crustal cross sections and xenolith localities. Proportions of the crustal rocks were adjusted such that average velocities at all depths were matched with the average crustal velocity-depth curve. The model [*Christensen and Mooney*, 1995, Figure 19] consists of an upper granitic crust which becomes increasingly tonalitic with depth. At midcrustal regions of 15 to 25 km depth, major lithologies are amphibolite facies rocks, consisting of granitic gneiss, biotite (tonalitic) gneiss, and amphibolite. At greater depths, mafic granulite gradually becomes abundant with mafic garnet granulite present immediately above the Mohorovicic discontinuity. Using the Poisson's ratio averages of Table 3, we find that Poisson's ratio will vary with depth on this model from 0.253 in the upper crust to 0.279 in the lowermost crust, with a maximum value of 0.283 at a depth of 30 km. The average crustal Poisson's ratio for this 40-km-thick average continental crustal model is 0.265, in good agreement with the average Poisson's ratio of 0.27 observed by *Zandt and Ammon* [1995].

Conclusions

The new Poisson's ratio averages presented in this paper provide a modern database for evaluating seismological ob-

Table 6. Average Crustal Velocities (V_p, V_s), Velocity Ratios (V_p/V_s), and Poisson's Ratios (σ)

Crustal Type	V_p, km s^{-1}	V_s, km s^{-1}	V_p/V_s	σ	Reference
Oceanic crust, Samail Ophiolite, Oman	6.464	3.440	1.879	0.302	*Christensen and Smewing* [1981]
Oceanic crust, Bay of Islands Ophiolite, Newfoundland	6.608	3.494	1.891	0.306	*Christensen and Salisbury* [1982]
Arc crust, Kohistan, Pakistan	6.691	3.780	1.770	0.266	*Miller and Christensen* [1994]
Average continental crust	6.454	3.650	1.768	0.265	*Christensen and Mooney* [1995]

servations of P and S wave velocities in the crystalline crust. The rock values of Poisson's ratio at confining pressures above 200 MPa are shown to be primarily controlled by mineralogy. Plagioclase feldspar composition is important, as well as the Fe-Mg ratios of pyroxenes and olivine. Reasonable agreement exists between the Poisson's ratios of monomineralic rocks and those calculated from single-crystal elastic constants.

Emphasis has been placed on the correlation of Poisson's ratio with simple mineralogical and chemical variables, with the objective of interpreting crustal seismological data. Poisson's ratios of igneous rocks are shown to change systematically with mineralogy. Progressive metamorphism can also produce significant changes in Poisson's ratios, which correlate qualitatively with mineralogical changes. Rocks with SiO_2 contents between 55% and 75% show a linear decrease in Poisson's ratio with increasing weight percent SiO_2. It thus appears that measurements of upper continental crustal Poisson's ratios can provide valuable information on crustal chemistry in regions where mafic rocks are absent. Rocks with SiO_2 contents less than 55%, many of which are likely abundant lower crustal and upper mantle lithologies, however, have a wide range of Poisson's ratios, with no correlation with SiO_2 content.

Recently, there have been many valuable field studies of crustal Poisson's ratios using a variety of seismic techniques, including refraction and wide angle reflection studies [e.g., *Holbrook et al.*, 1988; *Boland and Ellis*, 1991], near-normal incidence reflection data [*Ward and Warner*, 1991; *Pratt et al.*, 1993], seismic tomography [*White et al.*, 1992], and teleseismic data [*Clarke and Silver*, 1993; *Zandt and Ammon*, 1995]. The significance of these and future studies will grow, especially when the field measurements are combined with laboratory studies to provide improved constraints on crustal composition necessary to better understand crustal genesis and evolution.

The newly presented rock Poisson ratio averages (Table 3), when combined with V_p measurements (Figure 8), can lead to improved predictions of composition from seismic field studies. Equations (3) and (4) show, however, that at present many refraction measurements are unlikely to provide much greater resolution in Poisson's ratio than ±0.02. Future field measurements must be designed to improve data quality. To accomplish this, it is desirable to conduct experiments which employ a variety of techniques at a single location. For example, the new teleseismic and vertical reflection methods, which measure velocity ratios very accurately, should be applied at the same locations as high-resolution wide-angle refraction measurements. Such studies will be of prime importance in increasing our knowledge of crustal petrology.

Acknowledgments. The manuscript was greatly improved by the perceptive reviews of Tom Brocher, Tom Pratt, Donald White, and Joel Johnston. Jianping Xu provided valuable technical support for this study. Financial support was provided by the Office of Naval Research and the National Science Foundation Continental Dynamics Program.

References

Alexandrov, K. S., and T. V. Ryzhova, Elastic properties of rock-forming minerals, 2, layered silicates, *Bull. Acad. Sci. USSR, Geophys. Ser.*, Engl. Transl., *11*, 871-875, 1961a.

Alexandrov, K. S., and T. V. Ryzhova, Elastic properties of rock-forming minerals, 1, pyroxenes and amphiboles, *Bull. Acad. Sci. USSR, Geophys. Ser.*, Engl. Transl., *9*, 1165-1168, 1961b.

Alexandrov, K. S., and T. V. Ryzhova, The elastic properties of crystals, *Sov. Phys. Crystallogr.*, *6*, 228-252, 1961c.

Alexandrov, K. S., and T. V. Ryzhova, Moduli of elasticity of pyrite, *Izv. Acad. Sci. USSR, Sibir. Br.*, *6*, 43-47, 1961d.

Alexandrov, K. S., T. V. Ryzhova, and B. P. Belikov, The elastic properties of pyroxenes, *Sov. Phys. Crystallogr.*, *8*, Engl. Transl., 589-591, 1964.

Bass, J. P., and D. J. Weidner, Elasticity of single-crystal orthoferrosilite, *J. Geophys. Res.*, *89*, 4359-4371, 1984.

Berry, L. G., and B. Mason, *Mineralogy*, 612 pp., W.H. Freeman, New York, 1959.

Birch, F., The velocity of compressional waves in rocks to 10 kilobars, 1, *J. Geophys. Res.*, *65*, 1083-1102, 1960.

Birch, F., the velocity of compressional waves in rocks to 10 kilobars, 2, *J. Geophys. Res.*, *66*, 2199-2224, 1961.

Boland, A. V., and R. M. Ellis, A geophysical model for the Kapuskasing uplift from seismic and gravity studies, *Can. J. Earth Sci.*, *28*, 342-354, 1991.

Braile, L. W., W. J. Hinze, R. R. B. von Frese, and G. R. Keller, Seismic properties of the crust and uppermost mantle of the conterminous United States and adjacent Canada, in *Geophysical Framework of the Continental United States*, edited by L. C. Pakiser, and W. D. Mooney, *Mem. Geol. Soc. Am. 172*, 655-680, 1989.

Bratt, S. R., and S. C. Solomon, Compressional and shear wave structure of the East Pacific Rise at 11°20'N: Constraints from three-component ocean bottom seismometer data, *J. Geophys. Res.*, *89*, 6095-6110, 1984.

Brocher, T. M., and N. I. Christensen, Seismic anisotropy due to preferred mineral orientation observed in shallow crustal rocks in southern Alaska, *Geology*, *18*, 737-740, 1990.

Christensen, N. I., Shear wave velocities in metamorphic rocks at pressures to 10 kilobars, *J. Geophys. Res.*, *71*, 3549-3556, 1966a.

Christensen, N. I., Elasticity of ultrabasic rocks, *J. Geophys. Res.*, *71*, 5921-5931, 1966b.

Christensen, N. I., The abundance of serpentinites in the oceanic crust, *J. Geol.*, *80*, 709-719, 1972.

Christensen, N. I., Seismic velocities, in *Handbook of Physical Properties of Rocks*, vol. 2, edited by R. S. Carmichael, pp. 1-228, CRC Press, Boca Raton, Fla., 1982.

Christensen, N. I., Measurements of dynamic properties of rock at elevated temperatures and pressures, in *Measurement of Rock Properties at Elevated Pressures and Temperatures*, edited by H. J. Pincus and E. R. Hoskins, pp. 93-107, Am. Soc. for Test. and Mater., Philadelphia, Pa., 1985.

Christensen, N. I., and D. M. Fountain, Constitution of the lower continental crust based on expertimental studies of seismic velocities in granulite, *Geol. Soc. Am. Bull.*, *86*, 227-236, 1975.

Christensen, N. I., and W. D. Mooney, Seismic velocity structure and composition of the continental crust: A global view, *J. Geophys. Res.*, *100*, 9761-9788, 1995.

Christensen, N. I., and M. H. Salisbury, Lateral heterogeneity in the seismic structure of the ocean crust inferred from velocity studies in the Bay of Islands ophiolite, Newfoundland, *Geophys. J. R. Astron. Soc.*, *68*, 675-688, 1982.

Christensen, N. I., and G. H. Shaw, Elasticity of mafic rocks from the Mid-Atlantic Ridge, *Geophys. J. R. Astron. Soc.*, *20*, 271-284, 1970.

Christensen, N. I., and J. D. Smewing, Geology and seismic structure of the northern section of the Oman ophiolite, *J. Geophys. Res.*, *86*, 2545-2555, 1981.

Christensen, N. I., and D. L. Szymanski, Origin of reflections from the Brevard fault zone, *J. Geophys. Res.*, *93*, 1087-1102, 1988.

Clarke, T. J., and P. G. Silver, Estimation of crustal Poisson's ratio from broad band teleseismic data, *Geophys. Res. Lett.*, *20*, 241-244, 1993.

Coleman, R. G., *Ophiolites*, 229 pp., Springer-Verlag, New York, 1977.

Detrick, R., J. Collins, R. Stephens, and S. Swift, In situ evidence for the nature of the seismic layer 2-3 boundary in oceanic crust, *Nature*, *370*, 288-290, 1994.

Duffy, T. S., and M. T. Vaughan, Elasticity of enstatite and its relationship to crystal structure, *J. Geophys. Res.*, *93*, 383-391, 1988.

Griffin, W. L., and W. Y. O'Reilly, Is the continental Moho the crust-mantle boundary?, *Geology*, *15*, 241-244, 1987.

Gutenberg, B., *Physics of the Earth's Interior*, 240 pp., Academic, San Diego, Calif., 1959.

Halleck, P. M., The compression and compressibility of grossular

garnet: A comparison of x-ray and ultrasonic methods, Ph.D. thesis, 82 pp., Univ. of Chicago, Chicago, Ill., 1973.
Hamilton, E. L., Shear-wave velocity versus depth in marine sediments: A review, *Geophysics, 41*, 985-996, 1976.
Hashin, Z., and S. Shtrikman, A variational approach to the theory of the elastic behavior of polycrystals, *J. Mech. Phys. Solids, 10*, 343-352, 1962.
Hearmon, R. F. S., The elastic constants of anisotropic materials, II, *Adv. Phys., 5*, 523-582, 1956.
Hess, H. H., History of ocean basins, in *Petrologic Studies (Buddington Volume)*, edited by A. E. J. Engel, H. L. James, and B. F. Leonard, pp. 599-620, Geol. Soc. of Am., Boulder, Colo., 1962.
Holbrook, W. S., P. Gajewski, A. Krammer, and C. Prodehl, An interpretation of wide-angle compressional and shear wave data in southwest Germany: Poisson's ratio and petrological implications, *J. Geophys. Res., 93*, 12,081-12,106, 1988.
Holbrook, W. S., W. D. Mooney, and N. I. Christensen, The seismic velocity structure of the deep continental crust, in *Continental Lower Crust*, edited by D. M. Fountain, R. Arculus, and R. Kay, pp. 21-43, Elsevier, New York, 1992.
Isaak, P. G., O. L. Anderson, T. Goto, and I. Suzuki, Elasticity of single-crystal forsterite measured to 1700 K, *J. Geophys. Res., 94*, 5895-5906, 1989.
Johnson, R. A., and K. A. Hartman, Upper crustal Poisson's ratio in the Colorado Plateau from multicomponent wide-angle seismic recording, in *Continental Lithosphere: Deep Seismic Reflections, Geodyn. Ser.*, vol. 22, edited by R. Meissner et al., pp. 323-328, AGU, Washington, D.C., 1991.
Johnston, J. E., and N. I. Christensen, Shear wave reflectivity, anisotropies, Poisson's ratios, and densities of a southern Appalachian Paleozoic sedimentary sequence, *Tectonophysics, 210*, 1-20, 1992.
Kanamori, H., and H. Mizutani, Ultrasonic measurements of elastic constants of rocks under high pressures, *Bull. Earthquake Res. Inst. Univ. Tokyo, 43*, 173, 1965.
Kandelin, J., and D. J. Weidner, The single-crystal elastic properties of jadeite, *Phys. Earth Planet. Inter., 50*, 251-260, 1988a.
Kandelin, J., and D. J. Weidner, Elastic properties of hedenbergite, *J. Geophys. Res., 93*, 1063-1072, 1988b.
Kern, H., Elastic-wave velocity in crustal and mantle rocks at high pressure and temperature: The role of the high-low quartz transition and of dehydration reactions, *Phys. Earth Planet. Inter., 29*, 12-23, 1982.
Kern, H., and A. Richter, Temperature derivatives of compressional and shear wave velocities in crustal and mantle rocks at 6 kbar confining pressure, *J. Geophys., 49*, 47-56, 1981.
Kumazawa, M., and O. L. Anderson, Elastic moduli. pressure derivatives, and temperature deriviative of single-crystal olivine and single-crystal forsterite, *J. Geophys. Res., 74*, 5961-5972, 1969.
Levien, L., D. J. Weidner, and C. T. Prewitt, Elasticity of diopside, *Phys. Chem. Miner., 4*, 105-113, 1979.
McSkimin, H. J., P. Andreatch Jr., and R. N. Thurston, Elastic moduli of quartz verses hydrostatic pressure at 25° and -195.8°C, *J. Appl. Phys., 36*, 1962-1632, 1965.
Miller, D. J., and N. I. Christensen, Seismic signature and geochemistry of an island arc: A multidisciplinary study of the Kohistan accreted terrane, northern Pakistan, *J. Geophys. Res., 99*, 11,623-11,642, 1994.
Pelselnick, L., and R. A. Robie, Elastic constants of calcite, *J. Appl. Phys., 34*, 2494, 2495, 1963.
Percival, J. A., D. M. Fountain, and M. H. Salisbury, Exposed crustal cross sections as windows on the lower crust, in *Continental Lower Crust*, edited by D. M. Fountain, R. Arculus, and R. Kay, pp. 1-43, Elsevier, New York, 1992.
Pratt, T. L., J. F. Mondary, L. D. Brown, N. I. Christensen, and S. H. Danbom, Crustal structure and deep reflector properties: Wide angle shear and compressional wave studies of the midcrustal Surrency Bright Spot beneath southeastern Georgia, *J. Geophys. Res., 98*, 17,723-17,735, 1993.
Reuss, A., Berechnung der Fliessgrenze von mischkristallen auf grund der blastizitatsbedingung fur einkristalle, *Z. Angew Math. Mech., 9*, 49-58, 1929.
Ringwood, A. E., and D. H. Green, An experimental investigation of the gabbro-eclogite transformation and some geophysical implications, *Tectonophysics, 3*, 383-427, 1966.
Ryzhova, T. V., Elastic properties of plagioclase, *Bull. Acad. Sci. USSR., Geophys. Ser.*, English Transl., *7*, 633-635, 1964.
Ryzhova, T. V., and K. S. Alexandrov, The elastic properties of potassium-sodium feldspars, *Bull. Acad. Sci. USSR, Geophys. Ser.*, Engl. Transl., *7*, 53-55, 1965.
Ryzhova, T. V., K. S. Alexandrov, and V. M. Korobkova, The elastic properties of rock-forming minerals, 5, additional data on silicates, *Bull. Acad. Sci. USSR., Earth Phys., 2*, Engl. Transl., 63-65, 1966.
Salisbury, M. H., and N. I. Christensen, The seismic velocity structure of a traverse through the Bay of Islands ophiolite complex, Newfoundland: An exposure of oceanic crust and upper mantle, *J. Geophys. Res., 83*, 805-817, 1978.
Schreiber, E., O. L. Anderson, and N. Soga, *Elastic Constants and Their Measurement*, 196 pp., McGraw-Hill, New York, 1973.
Soga, N., Elastic constants of garnet under pressure and temperature, *J. Geophys. Res., 72*, 4227-4234, 1967.
Spudich, P., and J. Orcutt, Petrology and porosity of an ocean crustal site: Results from wave form modeling of seismic refraction data, *J. Geophys. Res., 85*, 1409-1434, 1980.
Sumino, Y., The elastic constants of Mn_2SiO_4, Fe_2SiO_4, and $C0_2SiO_4$, and the elastic properties of olivine group minerals at high temperature, *J. Phys. Earth, 27*, 209-238, 1979.
Svetlov, I. L., A. I. Epistian, A. I. Krivko, A. I. Samoil, I. N. Odintsev, and A. P. Andreev, Anisotropy of Poisson's ratio of single crystals of nickel alloy, *Sov. Phys. Dokl., 33*, 771-773, 1988.
Swift, S. A., and R. A. Stephen, How much gabbro is in ocean seismic layer 3?, *Geophys. Res. Lett., 19*, 1871-1874, 1992.
Tarkov, A. P., and V. V. Vavakin, Poisson's ratio behavior in various crystalline rocks: Application to the study of the Earth's interior, *Phys. Earth Planet. Inter., 29*, 24- 29, 1982.
Vaughan, M. T., and S. Guggenheim, Elasticity of muscovite and its relationship to crystal structure, *J. Geophys. Res., 91*, 4657-4664, 1986.
Vaughan, M. T., and D. J. Weidner, The relationship of elasticity and crystal structure in andalusite and sillimanite, *Phys. Chem. Miner., 3*, 133-144, 1978.
Voigt, W., *Lehrbuch der Kristallphysik*, B.G. Teulner, Leipzig, Germany, 1928.
Wang, H., and G. Simmons, Elasticity of some mantle crystal structures, 3, Spessartite-almandine garnet, *J. Geophys. Res., 79*, 2607-2613, 1974.
Ward, G., and M. Warner, Lower crustal lithology from shear wave seismic reflection data, *Geodynamics, 22*, 343-349, 1991.
White, D. J., B. Milkereit, M. H. Salisbury, and J. A. Percival, Crystalline lithology across the Kapuskasing uplift determined using in situ Poisson's ratio from seismic tomography, *J. Geophys. Res., 97*, 19993-20006, 1992.
Wilkens, R., G. Simmons, and L. Caruso, The ratio V_p/V_s as a discriminant of composition for siliceous limestones, *Geophysics, 49*, 1850-1860, 1984.
Yardley, B. W., *An Introduction to Metamorphic Petrology*, 248 pp., John Wiley, New York, 1989.
Zandt, G., and C. J. Ammon, Poisson's ratio of Earth's crust, *Nature, 374*, 152-155, 1995.

N. I. Christensen, Department of Earth and Atmospheric Sciences, Purdue University, West Lafayette, IN 47907-1397.

(Received June 29, 1995; revised November 2, 1995;
accepted November 8, 1995.)